PEDESTRIAN DETECTION IN A VIDEO SEQUENCE USING HOG AND COVARIANCE METHOD

Bhuvanarjun. K. M[1], T. C. Mahalingesh[2]

[1]*M. Tech Student, Siddaganga Institute of Technology, Tumakuru, Karnataka (India)*

[2]*Associate Professor, Dept. of Electronics and Communication, Siddaganga Institute of Technology, Tumakuru, Karnataka (India)*

ABSTRACT

Visual surveillance is one of the most frequently admired areas of research in the field of image processing and computer vision. The concept of object detection and recognition has been explored rigorously in the last few decades. Object detection is a key step in any smart visual system because it provides the primitive information for logical perceiving of the video footage. The significance of object detection and recognition has been comprehended well in the fields of Visual Surveillance, Human-Computer Interaction, Advanced Driver Recognition System, Medical Imaging and many more. There exists a great deal of problems for which there exists no optimal solution, so we have made an effective effortin the same direction for obtaining the acceptable result. To develop a detection algorithm using various image processing techniques is the main aim of this paper. A method is proposed to improve the detection rate in videos using combination of algorithms. The algorithms used here are Histogram of Oriented Gradients (HOG) and Covariance based method. The proposed method shows improvement in detection time andthe detection rate as well.

Keywords*: *Covariance, Histogram Of Oriented Gradients (HOG), Image Processing,Pedestrian Detection, Visual Surveillance.

I. INTRODUCTION

Object detection is a key component for many video surveillance applications such as Advanced Driver Assistance System (ADAS), Human- Computer Interaction (for gesture recognition to implement smart home and offices), and Visual Surveillance (for recognition of cautious and distrusting activities), Medical Imaging (tumor detection and analysis of patients) and many more. It is necessary to make video surveillance system smart by making them fast, robust and reliable by developing suitable algorithms which provides the highest degree of solution. Also the latest innovations in the field of computing power, data storage and processing have made the arena of visual surveillance most interesting. There are number of problems which are associated with object and/or pedestrian detection such as non-rigid object structure, changing appearance of the object and the background, occlusions occurring due to other objects as well as itself and motion of the camera itself. Also the variation in appearance which is because of geographic variability, various poses, illumination and scaling of objects causes the additional challenges. The primitive factor which needs to be considered in such scenarios is the computation and detection time. Thus understanding and comprehending the scenes in a video is challenging problem which requires scientific innovation and statistical analysis and is a very fruitful domain with serious real world applications.

Object detection is fundamentally recognition of non – stationary objects in a video sequence i.e., basically identifying a moving object. This paper addresses the issue of object detection in occlusion and low illumination scenarios. The system adopted by combining HOG and Covariance based detection gives satisfactory results in pedestrian detection. The proposed method of detection is evaluated on standard database as well as the database obtained locally.

The rest of the paper is organized in the following manner: Section 2 presents the previous work carried out in the field of object detection using various algorithms. Section 3 provides information on the proposed method using combination of algorithms and Section 4 gives the detailed description of feature extraction, HOG and Covariance method. Experimental results are presented in Section 5.

II. LITERATURE SURVEY

Several algorithms have been published for the purpose of pedestrian detection in the past decades, which have provided the roadmap in the visual surveillance domain.

In [1] Na Shou et al., have proposed a region of interest based pedestrian detection system, which reduces the overall size of the image thus reducing the detection time and improving accuracy. Navneet Dalal et al.,[2] have proposed a method called as Histogram of Oriented Gradients(HOG) for pedestrian detection. HOG features are computationally efficient and no feature has been show to outperform HOG in pedestrian detection [3, 4, 5]. The combination of ROIs based HOG makes the algorithm efficient computationally and real time as well. Oncel Tuzel et al. have proposed region descriptor method which can be applied for object detection and classification, known as Covariance based method[6]. These covariance matrices are combination of various image features which consists of statistical and spatial information [7, 8]. Pedro Cortez-Cargill et al.,[9] have discussed the accuracies of various feature vectors used for calculating the covariance matrix and have suggested the features which reduces the computation time and thus resulting in better detection system. In [10], the authors have combined HOG and Optical flow for detection and tracking of humans thus emphasizing the scope of combination of algorithms.

III. OVERVIEW OF THE PROPOSED DETECTION SYSTEM

The overview of the proposed pedestrian detection system using HOG and Covariance based method is described in Fig. 1.In the beginning, to identify the foreground objects, background subtraction along with some morphological operations are performed. Once we separate background and foreground objects, dynamic region of interest is extracted. For the detection window obtained, HOG features and Covariance matrix are calculated. HOG features are calculated and are fed to the linear Support Vector Machine (SVM). The SVM classifies the given input as either human or non-human. For the same detection window, Covariance features are calculated simultaneously. Covariance matrix is generated by concatenating various features such as coordinates, gradients, norms etc. For the obtained Covariance matrix dissimilarity measure is calculated using the template of the human image already stored in the database and the given image. The dissimilarity measure indicates whether there exists the desired object or not. If both the algorithms give the output as human, only then the algorithm proceeds for detection. Since we are detecting the object until it is disappearing from the scene there is no need for separate tracking algorithm thus reducing the complexity.

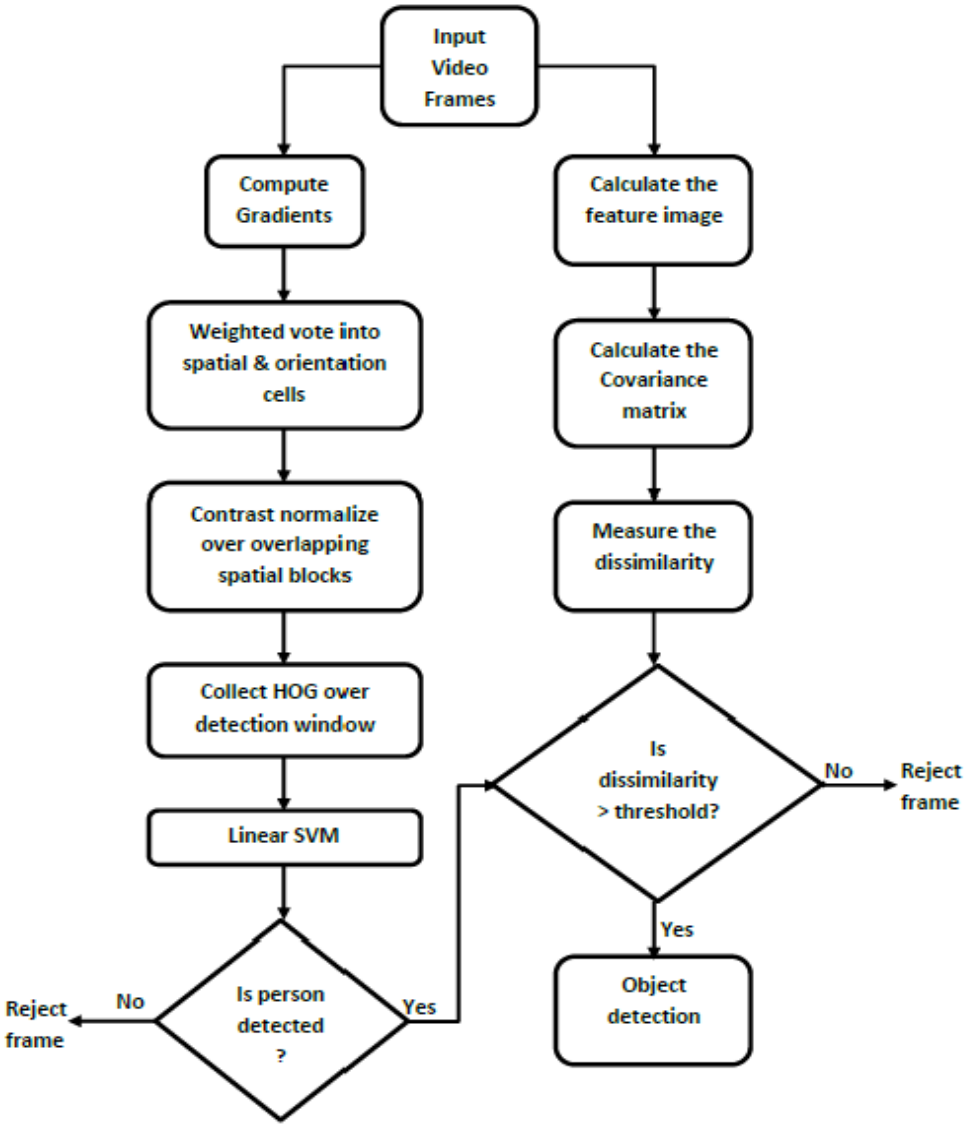

Figure 1. Overview of The Proposed Pedestrian Detection System Using HOG and Covariance Method

IV. DETECTION SYSTEM

In order to obtain the region of interest, the object in the foreground has to be localized as the work carried out in this methodology is for fixed camera. The foreground can be localized using the background subtraction algorithm. Here the background is initialized by considering a reference frame which does not have any object in it. Frame difference is calculated between the reference frame and the current frame which is shown in (1):

$$\text{Current\_frame} - \text{Reference\_frame} > \text{Threshold} \quad (1)$$

Only foreground objects will be available once we perform the background subtraction. By performing some morphological operations and using image thresholding, the background subtracted image will be converted into a binary image. The relevant figures are shown in Fig. 2.

(a) (b) (c)

Figure 2. Overview of Background subtraction stage (a) Reference frame (b) Current frame (c) Binarized image

For the image obtained after the background subtraction and thresholding, which is a binary image, region of interest is calculated. These interest points are nothing but the corners in both horizontal and vertical directions, which indeed corresponds to the variations in brightness levels. If the minimum of the two Eigen values of autocorrelation matrix of the second derivative of the image is greater than some predefined threshold then it will result in good corners, which is given by (2):

$$R = \text{Min}(|\lambda_1|,|\lambda_2|) > \lambda \quad (2)$$

Dynamic region of interest is created by plotting the interest points over a blank frame and a rectangle is drawn which bounds these interest points. The coordinates of the region of interest is mapped to the initial original gray image only if average intensity value is greater than the threshold. The extracted coordinates of region of interest is shown on Fig. 3. The detection algorithm is applied on this window.

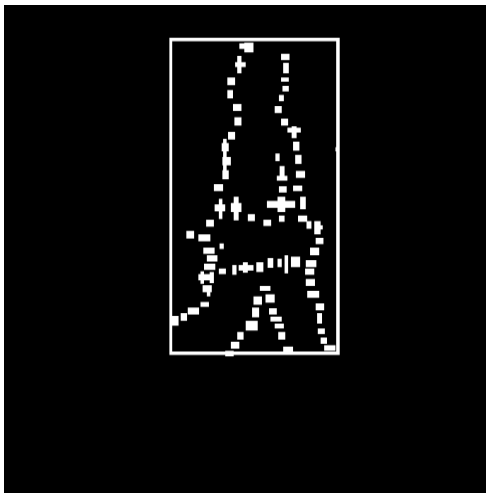

Figure 3. Dynamic Region of Interest Around Corner Points

4.1 Histogram of Oriented Gradients

The HOG features are very suitable for pedestrian detection as they are robust and give efficient performance. The HOG features are computed for the window size of 64 x 128 pixels, known as detection window. The detection window will be shifted throughout the entire image using full comprehensive scanning. To calculate the HOG features for each detection window, derivatives are calculated along both x and y directions using the 1-D derivative masks given by M_x=[-1,0,1] and M_y=[-1,0,1]^T. The derivative masks are convolved with the original image I which results in gradients in x and y direction is given by:

$$G_x = I * M_x \quad (3)$$

$$G_y = I * M_y \quad (4)$$

The gradient magnitude and orientation angle are calculated as:

$$|G(x, y)| = \sqrt{(G_x^2 + G_x^2)} \quad (5)$$

$$\varphi(x, y) = \arctan \frac{G_y}{G_x} \quad (6)$$

The orientation bins are spaced evenly over 0^0 - 360^0 or 0^0 – 180^0 based on signed or unsigned gradient values respectively. Here 9 bins are created with 20^0 for each bin with 0^0 – 180^0 unsigned gradient value.The 64 x 128 image is divided into a closely compacted grid. In this dense grid each unit of 8 x 8 pixels is called a cell. A group of 4 adjacent cells is called a block. Next step is to create cell histograms. Weighted votes are calculated for each orientation angle among all the pixels present in a cell. This orientation gives the direction of the edges passing through that particular pixel. A 9-D histogram is created for each cell. This in turn will result in a 9 x 4 = 36-D histogram for each block. Next block is considered for HOG feature calculation by extending 50% over the adjacent blocks. Thus in total 7 horizontal blocks and 15 vertical blocks, this sums to 7 x 15 = 105 blocks and is depicted in Fig. 4. The computed histogram is normalized to take care of illumination abnormalities. Finally the HOG feature vector is created by concatenating all the histograms in the entire image for all the blocks i.e., 105 x 36 = 3780 length feature vector. The histograms are normalized using L2-norm.

4.2 Covariance Method

Covariance based object detection is a simple and efficient method. An object is represented in terms of its statistical and spatial information. The Covariance matrix provides a way for combining various kind of information such as the modalities and the features of the given image.

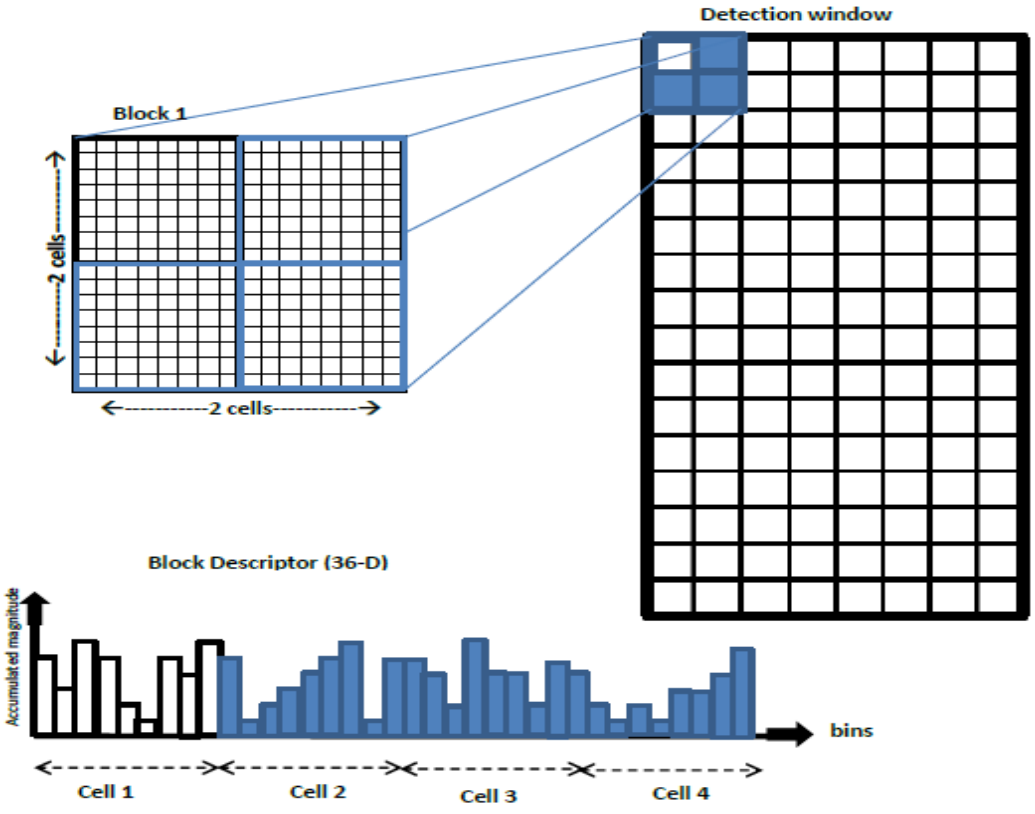

Figure 4. HOG Computation Block Descriptor

Let I be the given input image. Let W x H x d dimensional feature image be F, extracted from the input image I, and F is given by:

$$F(x, y) = \phi(I, x, y) \quad (7)$$

where ϕ can be any mapping such as color, gradient, norm, filter responses, coordinates etc.

For a given region of rectangularshape $R \subset F$, let $\{z_k\}_{k=1,2..n}$ be the d-dimensional feature points inside R.

The region R with d x d matrix of covariance of the feature points is given as:

$$C_R = \frac{1}{n-1}\sum_{k=1}^{n}(z_k - \mu)(z_k - \mu)^T \quad (8)$$

where μ represents the mean of the points.

The frequently used machine learning methods do not hold good for Covariance matrices as they do not lie in Euclidean space. The distance between the feature vectors is calculated using the nearest neighbor algorithm. The distance measure used to measure the dissimilarity between the two covariance matrices is given by:

$$\rho(C_1, C_2) = \sqrt{\sum_{i=1}^{n} \ln^2 \lambda_i(C_1, C_2)} \quad (9)$$

where $\{\lambda_i(C_1, C_2)\}_{i=1,2..n}$ are the generalized eigen values of C_1, C_2, computed from

$$\lambda_i C_1 x_i - C_2 x_i = 0 \quad i = 1...d \quad (10)$$

and $x_i \neq 0$ are the generalized eigen vectors.

The dimension of covariance matrices are very low i.e., it has only $(d^2 + d) / 2$ different values. The diagonal values present in the covariance matrix are the variance of the each feature and the correlations is represented by non-diagonal values.

In this methodology, a 7-D feature vector using pixel locations (x, y) and norm of the first and second order derivatives of the intensities with respect to x and y is calculated using (7).

V. EXPERIMENTAL RESULTS

In this section we have presented the experimental results of the proposed methodology. The proposed algorithm is implemented using OpenCV 2.4 on Microsoft Visual Studio 2010 IDE. The work is carried out in PC Intel Core i3 second generation CPU @ 2.13GHz processor and 3GB RAM. The size of the video frame is 320 x 240. The results obtained using the proposed method is satisfactory. The average time taken to detect the object using the proposed method is only 120 ms which is enough for real-time implementation.

The result of the proposed system is shown in Fig. 5. Also the detection rate can be improved in low illumination conditions by applying a new 1-D kernel [-1, 1, 2]. This kernel enhances the edge pixels while giving a fade-out or washed out look on the given image. The result of this method is shown in Fig. 6.

Figure 5. Pedestrian Detection using HOG and Covariance Method

Figure 6. Pedestrian Detection Using HOG and Covariance Method and Using 1-D Kernel

VI. CONCLUSION

In this paper we have proposed pedestrian detection system in a video sequence using HOG and Covariance based method. The pedestrian detection system is developed with less complexity and yields good detection rate with reduced detection time. The main contribution of this paper is combination of algorithms which reduces the false detection rate and also solves the problem of occlusion thus improving the efficiency. The conducted experiments have shown satisfying results in detection.

Further work of detection can be extended for multiple cameras in densely occluded and cluttered scenarios.

REFERENCES

[1] Na Shoul, Hong Peng, Hui Wang, Li-Min Meng and K.-L. Du, “An ROIs Based Pedestrian Detection System for Single Images”, IEEE 5th International Congress on Image and Signal Processing, 2012

[2] N. Dalal and B. Triggs, "Histograms of Oriented Gradients for Human Detection", IEEE Conference on Computer Vision and Pattern Recognition, vol. 1, pp. 886 - 893, 2005.

[3] M. Ishikawa et aI, "Selection of Histograms of Oriented Gradients Features for Pedestrian Detection", ICONIP 2007, Part II, LNCS 4985, pp. 598-607,springer-Verlag Berlin Heidelberg, 2008.

[4] P. Dollar, C. Wojek, B. Schiele, P. Perona, “Pedestrian detection: an evaluation of the state of the art,” IEEE Trans. Pattern Anal. Machine Intell., vol. 34, pp. 743-761, April ,2012.

[5] Daimeng Wei, Yong Zhao, Ruzhong Cheng and Guoliang Li, "An Enhanced Histogram of Oriented Gradient for Pedestrian Detection", Fourth International Conference on Intelligent Control and Information Processing (ICICIP), Beijing, China, June 2013.

[6] O. Tuzel, F. Porikli, and P. Meer, “Region covariance: A fast descriptor for detection and classification", In Proc. 9th European Conf. on Computer Vision, Graz, Austria, volume 2, pages 589-600, 2006.

[7] Yaping Liu, Jian Yao, Renping Xie, and Sa Zhu, “Pedestrian Detection from Still Images Based on Multi-Feature Covariances”, Proceeding of the IEEE International Conference on Information and AutomationYinchuan, China, August ,2013

[8] Prajna Parimita Dash, Santhosh Aitha and Dipti Patra,” Ohta Based Covariance Technique for Tracking Object in Video Scene”, IEEE Students’ Conference on Electrical, Electronics and Computer Science (SCEECS), Bhopal, India, Pages 1-4, March,2012

[9] Cargill P. C, Rius C. U, Domingo Mery and Alvaro Soto, “Performance Evaluation of the Covariance Descriptor for Target Detection”, International Conference of the Chilean Computer Science Soceity (SCCC), Santiago, Chile, , pages 133 – 141, Nov 10-12, 2009.

[10] Dayanand Kumar N. C, K. V Suresh, “HOG-PCA Descriptor with Optical Flow based Human Detection and Tracking", International Conf. on Communication and Signal Processing, April 3-5, 2014.

AN AUTHENTICATION SYSTEM FOR AN IMAGE: SECRET MOSAIC IMAGING AND LSB SUBSTITUTION

Deepak.A.B.C[1], P.S.Shilpashree[2]

[1]*M.Tech Student, Siddaganga Institute of Technology, Tumakuru, Karnataka, (India)*

[2]*Assistant Professor, Dept. of Electronics and Communication, Siddaganga Institute of Technology, Tumakuru, Karnataka, (India)*

ABSTRACT

Authentication of Color Images in present world is the most challenging task for Image Processing engineers and cryptographers because of its redundancy and spatial correlation. In this paper we have implemented an approach for image authentication in disguise of another image using color transformation technique and mosaicking image. We have used simple LSB substitution for hiding data required for image recovery in the receiver side. A good experimental result is shown for the feasibility of the methodology.

Keywords: Color Transformation, Mosaic Image, Data Hiding, LSB Substitution.

I. INTRODUCTION

Image has a natural property of spatial correlation and high data redundancy. By using these properties of the image researchers worked on authenticating the image. Image Encryption algorithms make use of these natural properties of the image to authenticate the image. The authenticated image may arouse an attacker's attention to decrypt the image because of its high redundancy. Another method of authenticating the color image is data hiding where we use two types of entities to transmit the image secretly. One is an image which we required to transmit secretly called as secret image and another one is an image which is used to hide the secret image called as a carrier image. These encryption and decryption process is controlled by key at transmitter and receiver end. Without the key we cannot decrypt the image at receiver end.

Several data hiding techniques have been proposed in the literature includes LSB Substitution [1], histogram Shifting [2], difference expansion [3], prediction error expansion [4].

In this paper we have implemented an authentication system for an image which transforms a secret image into meaningful mosaic image which looks like a preselected carrier image. We are using a simple LSB Substitution to hide the data required for recovering secret image at receiver end. The method implemented in this paper is inspired by Lai and Tsai [5] and Lee and Tsai [6]. The mosaic image is the result of rearrangement of the fragments of a secret image in disguise of another image called the carrier image preselected from a preselected database.

The implementation method in this paper yields the result shown in Fig. 1. Specifically, a secret image and a carrier image first divided into rectangular fragments and then the secret image blocks is fit into carrier image

blocks according to a similarity criterion based on color variations. Next, the color characteristic of each secret image block is transformed to be that of the corresponding carrier block in the carrier image, resulting in a mosaic image which looks like the carrier image. The relevant information required for recovering the original image id hide into the created mosaic image. The image encryption algorithms yield a mosaic image which is meaningless. The data hiding method must be hide data in highly compressed manner into a disguising mosaic image without compression.

(a) (b) (c)

Fig.1.1: Result Yielded by the Implementation. (A) Secret Image. (B) Carrier Image. (C) Secret-Fragment-Visible Mosaic Image Created From (A) And (B) by The Implementation.

In the remainder of this paper, the idea of the implementation is described in Sections 2. In Section 3 we have discussed about the creation of secret fragment visible mosaic image. In Section4, experimental results are presented to show the feasibility of the method, and in Section 5, the security considerations of the implementation and Section 6 is followed by conclusion and Section 7 is Scope for the future work.

II. METHODOLOGY

Taking merits of [5] [6] we have implemented a method for authentication of image. The block diagram of the implementation is shown in Fig. 2.

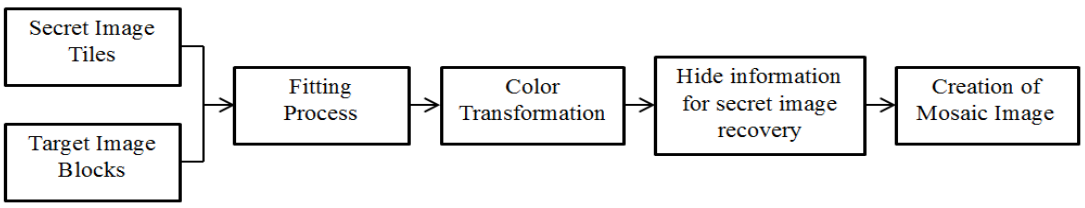

Fig. 2.1: Secret Fragment Mosaic Image Creation.

The implementation requires LSB substitution for data hiding discussed inChapter 2. The implementation includes two main phases as shown by the flow diagram of Figure. 3:1 and Figure. 3:2: 1) Mosaic image creation and 2) Secret image recovery.

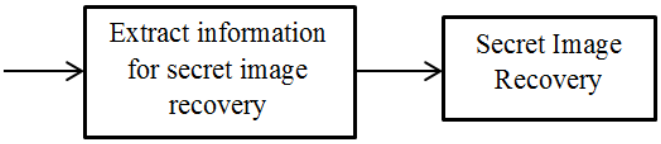

Fig. 2.2: Secret Image Recovery

In the first phase, a mosaic image is yielded, which consists of the fragmentsof an input secret image with color corrections according to a similarity criterion based on color variations. The phase includes three stages:

1. Fitting the tile images of the secret image into the target blocks of a preselected target image;
2. Transforming the color characteristic of each color channel in tile image of the secret image to become that of the corresponding color channel of target block in the target image;
3. Embedding relevant information into the created mosaic image for futurerecovery of the secret image using simple LSB Substitution.

In the second phase, the embedded information is extracted to recover nearly losslessly the secret image from the generated mosaic image. The phase includes two stages:

1. Extracting the embedded information for secret image recovery from the mosaic image,
2. Recovering the secret image tiles using the extracted information.

III. PROCESS OF CREATION OF MOSAIC IMAGE

3.2 Steps for Creating Mosaic Secret Fragment Visible Mosaic Image

1. Divide the secret S into n tile images and target image T into n target blocks.
2. Compute mean and standard deviation of each tile and block for three color channels according to following relations.

$$\mu_c = \frac{1}{n}\sum_{i=1}^{n} c_i, \qquad \mu_c^{'} = \frac{1}{n}\sum_{i=1}^{n} c_i^{'} \tag{1}$$

$$\sigma_c = \sqrt{\frac{1}{n}\sum_{i=1}^{n}(c_i - \mu_c)^2}, \qquad \sigma_c^{'} = \sqrt{\frac{1}{n}\sum_{i=1}^{1}(c_i^{'} - \mu_c^{'})^2} \tag{2}$$

In which and denote the C-channel values of pixels Tile imagesand target blocks respectively, with $c = r, g,$ or b and C=R, G, or B.

3. Sort the tile image and target blocks according to standard deviation and 3 color channels, after that we get we get new tile images and target blocks and note down the indices values of the color pixels.
4. After we get the new tile images and target blocks and compute the average standard deviation of these tile images and target blocks.
5. Fit the tile images and target blocks according to average standard deviation and create mosaic image according to the indices values.
6. Perform the Color transformation according to the new tile images and target blocks according to the following equations.

   New Color Values is find out by

$$c_i^{''} = q_c(c_i - \mu_c) + \mu_c^{'} \tag{3}$$

It is observed that the new color mean and standard deviation values are equal to the Target blocks.

standard deviation quotient cannot be zero because the original pixel value cannot be recovered back.

The original values can be reconstructed by the following equation

$$c_i = \frac{1}{q_c}(c_i^{''} - \mu_c^{'}) + \mu_c \tag{4}$$

7. Embed the secret image recovery information into the Mosaic Image i.e., indices of location, mean of the target block and tile image and standard deviation using LSB substitution. .

3.2 Secret Image Recovery

1. At the receiving end extract the LSB bits.
2. Retrieve the Tile Images according to LSB bits Hidden at the transmitter end according to (4).

IV. EXPERIMENTAL RESULTS

We have conducted several experiments on several images of size 512 512 divided into 4 4. The Results of the implementation is shown in the following figures.

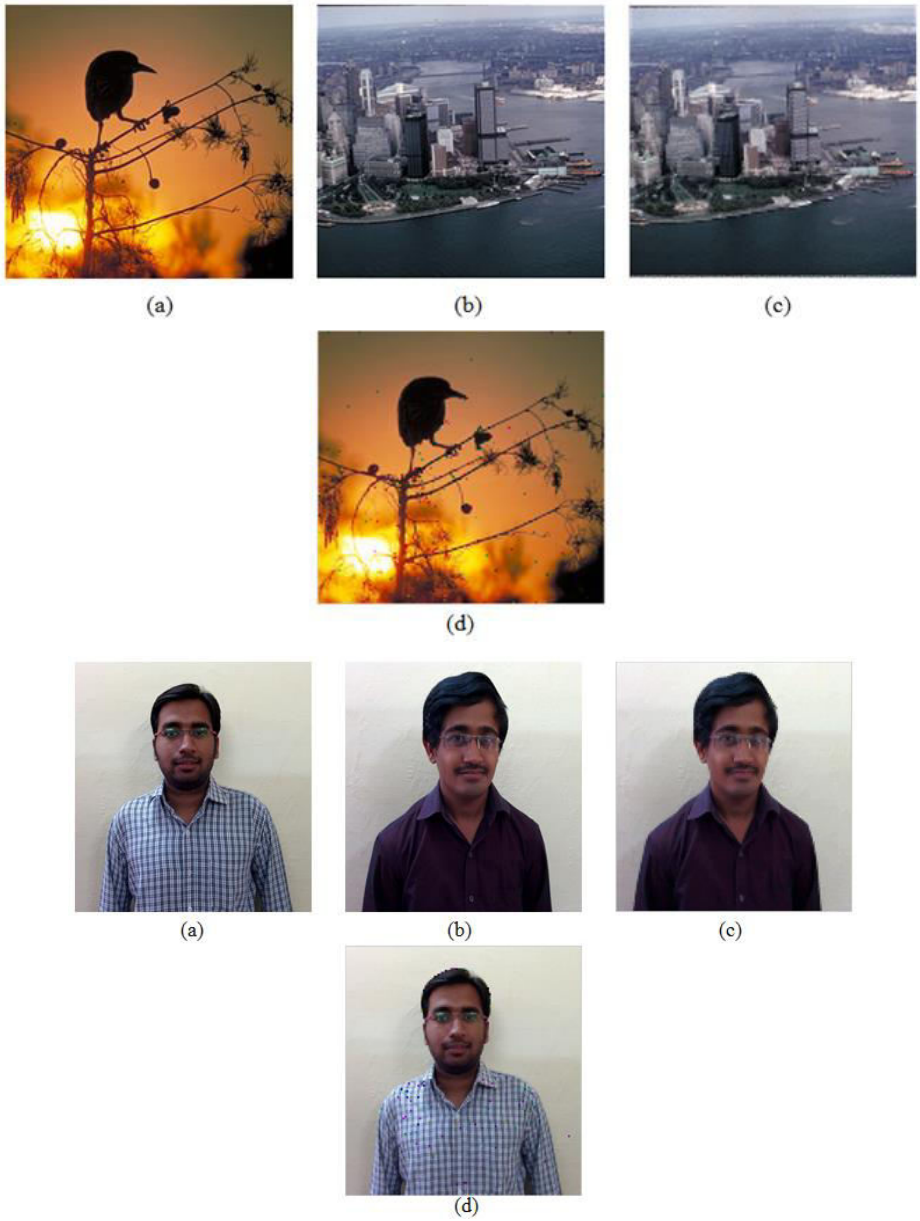

Fig. 4.1: (A) Secret Image, (B) Target Image, (C) Created Secret Fragment Visible Mosaic Image, (D) Recovered Secret Image from Mosaic Image

We have collected some medical image database for the secret image transmission as shown in the figure below. The medical image database may be secretly transmitted without distortion. The database is collected from a dermatologist having skin disease. The results are shown in the Figure 4.2.

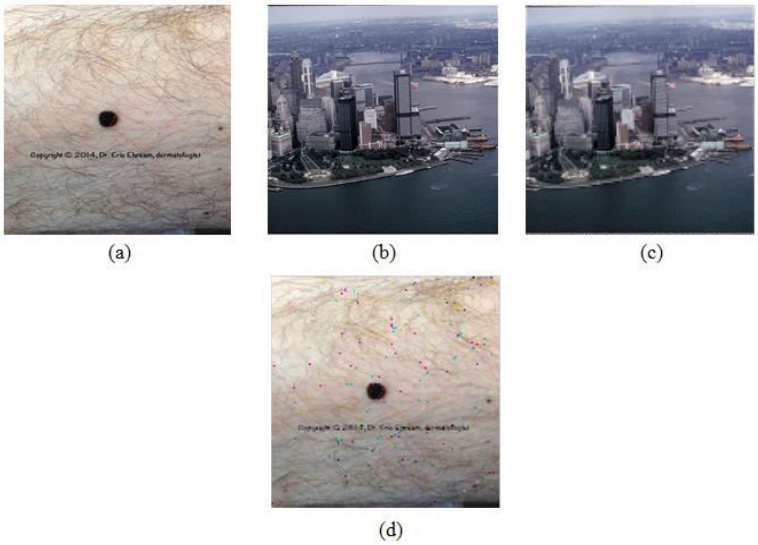

Fig. 4.2:(a) Pigmented lesion in Skin,(b) Target Image, (c) Mosaic Image,(d) Recovered Image (Courtesy: Dr. Eric Ehrsam (Dermatologist))

V. SECURITY ISSUES

In order to increase the security of the implementation of the authentication system, the embedded information for later recovery is encrypted. Only the receiver who has the decryption algorithm can recover the secret image. However, an eavesdropper who does not have the key may still try all possible permutations of the tile images in the mosaic image to get the secret image back. Fortunately, the number of all possible permutations here is $n!$, and so the probability for him/her to correctly guess the permutation is $p = 1/n!$ which is very small in value. For example, for the typical case in which divide a secret image of size 512×512 into tile images with block size 4×4, the value n is $(512 \times 512)/(4 \times 4) = 16{,}384$. So the probability to guess the permutation correctly is $1/n! = 1/16{,}384!$ So breaking the system by thisway of guessing is computationally infeasible.

Furthermore, even if one happens to guess the permutation correctly, such as the correctly guessed permutations, he/she still does not know the correct parameters for recovering the original color appearance of the secret image because such parameter information for color recovery is encrypted as a bit stream. Even so, it still should be assumed, in the extreme case, that he/she will observe the content of the mosaic image with a correct permutation, and try to figure useful information out of it. For example, an attacker might analyze the spatial continuity of the mosaic image in order to estimate a rough version of the secret image.

VI. CONCLUSION

The feasible and robust algorithm for image authentication is implemented andsecurity considerations of the algorithms are discussed. The authentication methods are based on creation of secret fragment visible mosaic image data and LSBsubstitution data hiding. The quality metrics of extracted secret image from thesecret

fragment mosaic image is shown. The parameters considered for data hidingare indices of the secret blocks, mean and standard deviation quotient discussedin Chapter 3. The method can create meaningful mosaic images but also cantransform a secret image into a mosaic one with the same data size for use as acamouflage of the secret image. The original secret images can be recovered nearlylosslessly from the created mosaic images. The $l\alpha\beta$ color space is used for colortransformation of secret image and cover image. It ensures to embed large imagedata into secret fragment visible mosaic image.

VII. SCOPE FOR FUTURE WORK

The algorithm for image authentication is implemented in MATLAB 2012a. For better speed and still more security reasons the algorithmcan be implemented in Open CV. In the implementation the key is not embedded into the secret fragment visible mosaic image. If this could be done the security consideration of the algorithms still improves. Without key recover the secretimage from secret fragment visible mosaic image. The secret fragment mosaic image is meaningless file without key at that instance. In the methodology the secret image is not correctly recovered from secret fragment visible mosaic image. If it is recovered correctly it shows the feasibility of the implementation.

REFERENCES

[1] C. K. Chan and L. M. Cheng, “Hiding data in images by simple LSB substitution,” Pattern Recognition..,vol. 37, pp. 469474, Mar. 2004.

[2] Z. Ni, Y. Q. Shi, N. Ansari, and W. Su, “Reversible data hiding,” IEEE Trans. Circuits Syst. Video Technol., vol. 16, no. 3, pp. 354362, Mar. 2006.

[3] J. Tian, “Reversible data embedding using a difference expansion,” IEEE Trans. Circuits Syst. Video Technol., vol. 13, no. 8, pp. 890896, Aug. 2003.

[4] V. Sachnev, H. J. Kim, J. Nam, S. Suresh, and Y.-Q. Shi, “Reversible water- marking algorithm using sorting and prediction,” IEEE Trans. Circuits Syst. Video Technol., vol. 19, no. 7, pp. 989-999, Jul. 2009.

[5] I. J. Lai and W. H. Tsai, “Secret-fragment-visible mosaic image—A new computer art and its application to information hiding,” IEEE Trans. Inf. Forens. Secur., vol. 6, no. 3, pp. 936–945, Sep. 2011.

[6] Ya-Lin Lee and Wen-Hsiang Tsai, “A New Secure Image Transmission Technique via Secret-Fragment-Visible Mosaic Images by Nearly Reversible Color Transformations,” IEEE Trans. Circuits and systems for video technology., volume:24 , Issue: 4 ,pp. 695 – 703, April 2014.

FINGERPRINT IMAGE ENHANCEMENT AND COMPARISON OF METHODS TO LOCATE VALID MINUTIAE

Sumitha.S.M[1], A.N.Mukunda Rao[2]

[1]PG Scholar, [2]Associate Professor, Dept. of Electronics and Communication,
Siddaganga Institute of Technology, Tumkur,Karnataka, (India)

ABSTRACT

This paper presents a method to improve quality of fingerprint image before extracting minutiae points from image. Also it compare the two approaches for false minutiae removal. Fingerprint image undergoes pre-processing steps which include normalisation, segmentation, orientation estimation, freuency estimation, Gabor filtering, binarization and thinning. Crossing number method is used for minutiae extraction. False minutiae removal is done based on average inter-ridge distance and based on connected component labeling. Implementation is done in Visual studio 2010 in C++ language using OpenCV libraries.

Keywords: Enhancement, Fingerprint, False Minutiae, Minutiae, Segmentation

I. INTRODUCTION

Fingerprint identification is one of the most important biometric technologies which have been used in many areas like security, forensics, banking etc. A fingerprint is the pattern of ridges and valleys on the surface of a fingertip. Fingerprints are unique for each individual and remains same throughout the life. User acceptability is higher for fingerprint identification. Challenges involved in fingerprint identification are: (i)High displacements/rotation, (ii)Distortion, (iii)Different pressure and skin conditions, (iv)Feature extraction errors. These may result in spurious or missing features. So, there is requirement for efficient fingerprint enhancement technique to remove noise and improves the clarity of ridges and valleys. The one of the local ridge characteristics is minutiae. There are two types of minutiae points one is ridge ending and other is ridge bifurcation. A ridge ending is defined as the point where a ridge ends abruptly. A ridge bifurcation is defined as the point where a ridge forks or diverges into branch ridges. A good quality fingerprint typically contains about 40–100 minutiae.

A critical step in Automatic Fingerprint matching system is to automatically and reliably extract minutiae from input finger print images. However the performance of the Minutiae extraction algorithm relies heavily on the quality of the input fingerprint image. In order to ensure to extract the true minutiae points it is essential to incorporate the enhancement algorithm. There are two ways in which we can enhance the input fingerprint image. 1. Binarization method. 2. Direct gray-level enhancement. The steps included in Binarization method are local histogram equalization, Wiener filtering, Binarization and thinning. The steps included in direct gray-level enhancement are normalization, orientation estimation, frequency estimation and filtering. Usually crossing number method is used to locate minutiae points.

II. FINGERPRINT ENHANCEMENT

Fingerprint image is captured using fingerprint scanner. Fingerprint image contains noise due to scanner, different pressure or skin conditions. So, it is not suitable to directly extract the features. It has to be enhanced before feature extraction.

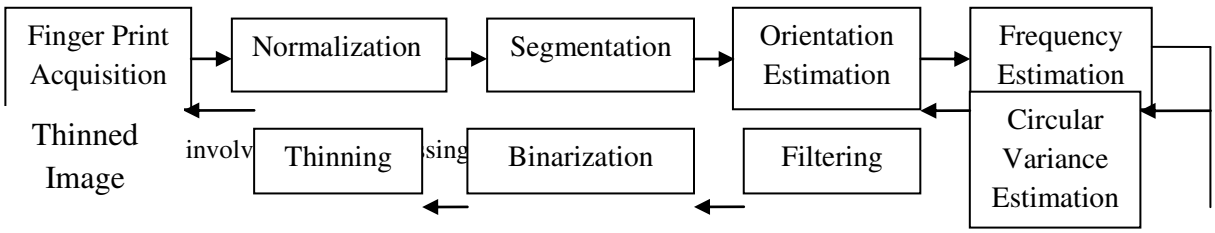

2.1 Normalization

Let $I(i,j)$ denote the gray level value of the pixel (i,j) for an $N \times N$ image. The mean M and variance VAR is given by the equations (1) and (2) respectively. Let $G(i,j)$ denotes the normalized gray level value at pixel(i,j), M_0 and VAR_0 are desired mean and variance values respectively, then the normalized image is defined as in the equation (3). Normalization doesn't change the clarity of ridge and valley structures. The main purpose of normalization is to reduce the variations in the gray level values along ridges and valleys [1].

$$M(I) = \frac{1}{N^2}\sum_{i=0}^{N-1}\sum_{j=0}^{N-1} I(i,j) \quad (1)$$

$$VAR(I) = \frac{1}{N^2}\sum_{i=0}^{N-1}\sum_{j=0}^{N-1} (I(i,j) - M(I))^2 \quad (2)$$

$$G(i,j) = \begin{cases} M_0 + \sqrt{\frac{VAR_0 (I(i,j) - M)^2}{VAR}} & if\ I(i,j) > M \\ M_0 - \sqrt{\frac{VAR_0 (I(i,j) - M)^2}{VAR}} & otherwise \end{cases} \quad (3)$$

2.2 Segmentation

Segmentation is the process of separating the foreground regions in the image from the background regions. The foreground regions correspond to the clear fingerprint area containing the ridges and valleys, which is the area of interest. The background corresponds to the regions outside the borders of the fingerprint area, which do not contain any valid fingerprint information. When minutiae extraction algorithms are applied to the background regions of an image, it results in the extraction of noisy and false minutiae. Thus, segmentation is employed to discard these background regions, which facilitates the reliable extraction of minutiae.

In a fingerprint image, the background regions generally exhibit a very low grey-scale variance value, whereas the foreground regions have a very high variance. Hence, a method based on variance thresholding can be used to perform the segmentation [2]. Firstly, the image is divided into blocks and the grey-scale variance is calculated for each block in the image. If the variance is less than the global threshold, then the block is assigned to be a background region. Otherwise, it is assigned to be part of the foreground.

2.3 Orientation estimation

The orientation field of a fingerprint image defines the local orientation of the ridges contained in the fingerprint. The orientation estimation is a fundamental step in the enhancement process as the subsequent Gabor filtering stage relies on the local orientation in order to effectively enhance the fingerprint image. The least mean square estimation method is used to compute the orientation image [1]. The steps for calculating the orientation at pixel (i,j) are as follows:

(1) Input image I is divided into non-overlapping blocks of size $w \times w$.

(2) The gradients $\partial_x(i,j)$ and $\partial_y(i,j)$ at each pixel (i,j) are computed. The gradient operator may vary from simple *Sobel* operator to more complex *Marr Hildreth* operator.

(3) The local orientation of each block centered at pixel (i,j) is estimated using the following equations.

$$V_x(i,j) = \sum_{u=i-w/2}^{i+w/2} \sum_{v=j-w/2}^{j+w/2} 2\,\partial_x(i,j)\partial_y(i,j) \quad (4)$$

$$V_y(i,j) = \sum_{u=i-w/2}^{i+w/2} \sum_{v=j-w/2}^{j+w/2} \left(\partial_x^2(u,v) - \partial_y^2(u,v)\right) \quad (5)$$

$$\theta(i,j) = \frac{1}{2}\tan^{-1}\left(\frac{V_y(i,j)}{V_x(i,j)}\right) \quad (6)$$

Where $\theta(i,j)$ is the least square estimate of the local orientation at the block centered at pixel (i,j).

(4) Smooth the orientation field in a local neighborhood using a Gaussian filter. The orientation image is firstly converted into a continuous vector field, which is defined as:

$$\emptyset_x(i,j) = \cos(2\,\theta(i,j)) \quad (7)$$

$$\emptyset_y(i,j) = \sin(2\,\theta(i,j)) \quad (8)$$

Where $\emptyset_x$ and $\emptyset_y$ are the *x* and *y* components of the vector field, respectively.

(5) After the vector field has been computed, Gaussian smoothing is then performed as follows:

$$\emptyset_x'(i,j) = \sum_{u=-w_\emptyset/2}^{w_\emptyset/2} \sum_{v=-w_\emptyset/2}^{w_\emptyset/2} W(u,v).\emptyset_x(i-uw, j-vw) \quad (9)$$

$$\emptyset_y'(i,j) = \sum_{u=-w_\emptyset/2}^{w_\emptyset/2} \sum_{v=-w_\emptyset/2}^{w_\emptyset/2} W(u,v).\emptyset_y(i-uw, j-vw) \quad (10)$$

Where *G* is a Gaussian low-pass filter of size $w_\emptyset \times w_\emptyset$.

(6) The final smoothed orientation field O at pixel (i,j) is defined as:

$$O(i,j) = \frac{1}{2}\tan^{-1}\left(\frac{\emptyset_y'(i,j)}{\emptyset_x'(i,j)}\right) \quad (11)$$

2.4 Frequency estimation

In addition to the orientation, another important parameter that is used in the construction of the Gabor filter is the local ridge frequency. The frequency image represents the local frequency of the ridges in a fingerprint [1].

Let G and O be the normalized image and oriented image respectively, then the steps involved in local ridge frequency estimation are

(1) Divide G into blocks of size $w\ x\ w$.

(2) For each block centered at pixel (i,j) compute an oriented window of size $l\ x\ w$ and then compute the signature $X[0], X[1], X[2] \ldots\ldots\ldots X[l-1]$, the ridges and valleys within oriented window where

$$X[k] = \frac{1}{w}\sum_{d=0}^{w-1} G(u,v), \qquad k = 0,1,\ldots\ldots,l-1 \tag{12}$$

$$u = i + \left(d - \frac{w}{2}\right) cosO(i,j) + \left(k - \frac{l}{2}\right) sinO(i,j) \tag{13}$$

$$v = j + \left(d - \frac{w}{2}\right) sinO(i,j) + \left(\frac{l}{2} - k\right) cosO(i,j) \tag{14}$$

If no minutiae or singular points appear in the oriented window, the x-signature forms a discrete sinusoidal shape wave, which has the same frequency as that of the ridges and valleys in the oriented window. Therefore, the frequency of ridges and valleys can be estimated from the x-signature. Let $T[i,j]$ be the average number of pixels between two consecutive peaks in the x-signature, then the frequency $\Omega(i,j)$ computed as $\Omega(i,j) = \frac{1}{T(i,j)}$. If no consecutive peaks can be detected from the x-signature , then the frequency is assigned a value of -1 to separate it from the valid frequency values.

(3) For a fingerprint image scanned at a fixed resolution the value of the frequency of the ridges and valleys in a local neighborhood lies in a certain range. If the estimated value of the frequency is out of this range, then the frequency is assigned a value of -1 to indicate that the valid frequency cannot be obtained.

(4) The blocks in which minutiae and/or singular points appear and /or ridges and valleys are corrupted do not form a well-defined sinusoidal shaped wave. The frequency values for these blocks need to be interpolated from the frequency of the neighboring blocks which have a well-defined frequency. The interpolation is performed as follows:

(a)For each block centered at (i,j)

$$\Omega'(i,j) = \begin{cases} \Omega(i,j) & if\Omega(i,j) \neq -1 \\ \dfrac{\sum_{u=-w_n/2}^{w_n/2}\sum_{v=-w_n/2}^{w_n/2} W_g(u,v)\mu((i-uw, j-vw))}{\sum_{u=-w_n/2}^{w_n/2}\sum_{v=-w_n/2}^{w_n/2} W_g(u,v)\delta((i-uw, j-vw)+1)} & otherwise \end{cases} \tag{15}$$

Where,

$$\mu(x) = \begin{cases} 0 & if\ x \leq 0 \\ x & otherwise \end{cases} \tag{16}$$

$$\delta(x) = \begin{cases} 0 & if\ x \leq 0 \\ 1 & otherwise \end{cases} \tag{17}$$

Wg is a discrete Gaussian kernel with fixed mean and variance and w_n is the size of the kernel.

(b) If there exists at least one block with the frequency value of -1, then swap Ω and Ω' and repeat step(a).

(5) Inter-ridge distances change slowly in a local neighborhood. A low –pass filter can be used to remove the outliers occurred due to such changes.

$$F(i,j) = \sum_{u=-w_n/2}^{w_l/2}\sum_{v=-w_n/2}^{w_l/2} W_l(u,v)\Omega'(i-uw, j-vw) \tag{18}$$

Where, W_l is two dimensional low –pass filter and w_l is the size of the filter.

The configuration of parallel ridges and valleys with well-defined frequency and orientation in a fingerprint image provide useful information which helps in removing undesired noise. The sinusoidal –shaped waves of ridges and valleys vary slowly in a local constant orientation. Therefore a suitable band-pass filter that is tuned to the corresponding frequency and orientation may be used if necessary to remove the undesired noise and preserve the true ridge and valley structures.

2.5 Filtering

Once the ridge orientation and ridge frequency information has been determined, these parameters are used to construct the even-symmetric Gabor filter. A two dimensional Gabor filter consists of a sinusoidal plane wave of a particular orientation and frequency, modulated by a Gaussian envelope. Gabor filters are employed because they have frequency-selective and orientation-selective properties. These properties allow the filter to be tuned to give maximal response to ridges at a specific orientation and frequency in the fingerprint image. Therefore,

a properly tuned Gabor filter can be used to effectively preserve the ridge structures while reducing noise [1].

An even-symmetric Gabor filter has general form as:

$$h(X, Y: \emptyset, f) = exp\left\{-\frac{1}{2}\left[\frac{X_\emptyset^2}{\delta_X^2} + \frac{Y_\emptyset^2}{\delta_Y^2}\right]\right\} \cos(2\pi f X_\emptyset) \quad 19$$

$$X_\emptyset = X cos\emptyset + Y sin\emptyset \quad 20$$

$$Y_\emptyset = -X sin\emptyset + Y cos\emptyset \quad 21$$

Where, $\emptyset$ is the orientation of Gabor filter, f is the frequency of a sinusoidal plane wave, δ_X and δ_Y are the standard deviations of Gaussian envelope along X and Y axes, respectively.

Let G be normalized fingerprint image, O be the orientation image, F be the frequency image and S be the segmentation mask, the enhanced image E is obtained as follows:

$$E(i,j) = \begin{cases} 255 & if\ S(i,j) = 0 \\ \sum_{u=-w_g/2}^{w_g/2} \sum_{v=-w_g/2}^{w_g/2} h\big(u, v: O(i,j), F(i,j)\big) G(i-u, j-v) & otherwise \end{cases} \quad 22$$

Where, w_g is the size of Gabor filter.

2.6 Binarization

Binarization is the process that converts a grey level image into a binary image. This improves the contrast between the ridges and valleys in a fingerprint image and consequently facilitates the extraction of minutiae. A locally adaptive binarization method is performed. It is the mechanism of transforming a pixel value to1 if the value is larger than the mean intensity value of selected block. Otherwise it is 0.

2.7 Thinning

Thinning is a morphological operation that successfully erodes away the foreground pixels until they are one pixel wide. The thinning operation is done using two sub-iterations [3]. Each sub-iterations begins by examining the neighborhood of each pixel in the binary image and based on a particular set of pixel deletion criteria it

checks whether the pixel can be deleted or not. These sub-iterations continue until no more pixels can be deleted. It also preserves the connectivity of ridges. Guo-Hall thinning algorithm is used and steps are as follows:

P_9	P_2	P_3
P_8	P_1	P_4
P_7	P_6	P_5

(1) Calculate $C(P_1)$

$$C(P_1) = !P_2 \& (P_3 | P_4) + !P_4 \& (P_5 | P_6) + !P_6 \& (P_7 | P_8) + !P_8 \& (P_9 | P_2) \quad 23$$

It indicates the number of distinct 8-connected component of 1's in $P_1's$ 8-neighborhood.

(2) Calculate $N(P_1)$

$$N(P_1) = MIN[N_1(P_1), N_2(P_1)] \quad 24$$

where,

$$N_1(P_1) = (P_9 | P_2) + (P_3 | P_4) + (P_5 | P_6) + (P_7 | P_8) \quad 25$$

$$N_2(P_1) = (P_2 | P_3) + (P_4 | P_5) + (P_6 | P_7) + (P_8 | P_9) \quad 26$$

$N_1(P_1)$ and $N_2(P_1)$ each break the ordered set of $P_1's$ neighboring pixel into four pairs of adjoining pixels and count the number of pairs which contain one or two 1's.

(3) Calculate $(P_2 | P_3 | !P_5) | P_4$ for add iteration or $(P_6 | P_7 | !P_9) \& P_8$ for even iteration.

(4) Delete the pixel $P(i, j)$, if $C(P_1) = 1$ and $2 \leq N(P_1) \leq 3$ and

a. $(P_2 | P_3 | !P_5) | P_4 = 0$ for add iteration.

b. $(P_6 | P_7 | !P_9) \& P_8 = 0$ for even iteration.

(5) Carry out the step 1 to 4 for all the pixels in the image.

(6) If pixel is deleted, go back to step 1 else stop the thinning process.

III. MINUTIAE

Minutiae are the minute, precise and trivial details. These mainly include ridge endings and ridge bifurcations which are shown in figure (2).

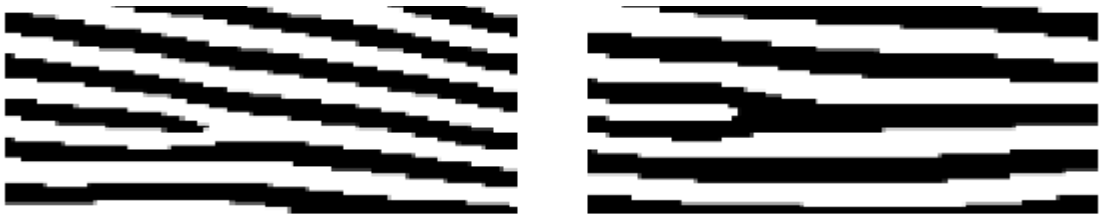

Figure 2: Left Ridge Ending and Right Ridge Bifurcation

3.1 Minutiae marking

The most commonly used method of minutiae extraction is the crossing number concept [4]. In this method, the thinned image is used where the ridge pattern is eight connected. The minutiae are extracted by scanning the local neighborhood of each ridge pixel in the eight-neighborhood. Using the properties of the crossing number

the ridge pixel can then be classified as a ridge ending, bifurcation or non-minutiae point. The crossing number CN for a ridge pixel P is given by,

$$CN = \frac{\sum_{i=1}^{8} |P_i - P_{i+1}|}{2} \quad (27)$$

Where, P_i is the pixel value in the neighborhood of P.

P_4	P_3	P_2
P_5	P	P_1
P_6	P_7	P_8

Figure 3: Order of Scan Around Pixel P

For a pixel$P$, its eight neighboring pixels are scanned as shown in figure (3). After obtaining the crossing number CN, minutiae are marked. If $CN = 1$ then pixel P is ridge ending point and if $CN = 3$ then pixel P is ridge bifurcation point.

3.2 Removal of False Minutiae Using Connected Component Labeling Approach

The pre-processing stage does not totally heal the fingerprint image. Through the scanned fingerprint image gets better clarity through pre-processing stage, each of all the earlier stages occasionally introduce some small amount of errors which later lead to spurious minutiae. Therefore removal of false minutiae is essential to keep the fingerprint verification system effective.

To removing false minutiae following steps are carried out for each candidate minutiae (ridge ending or ridge bifurcation)[5]:

1. Create and initialize with 0 an image L of size $W \times W$. Each pixel of L corresponds to a pixel of the thinned image which is located in a $W \times W$ neighborhood centered in the candidate minutia.

2. Label with -1 the central pixel of L (Figure (4a), Figure (5a)). This is the pixel corresponding to the candidate minutia point in the thinned ridge map image.

3. If the candidate minutia is a ridge ending then:

(a) Label with 1 all the pixels in L which correspond to pixels connected with the candidate ridge ending in the thinned ridge map image (Figure (4b)).

(b) Count the number of 0 to 1 transitions (T_{01}) met when making a full clockwise trip along the border of the L image (Figure (2c)).

(c) If $T_{01} = 1$, then validate the candidate minutia as a true ridge ending.

4. If the candidate minutia is a ridge bifurcation then:

(a) Make a full clockwise trip along the 8 neighborhood pixels of the candidate ridge bifurcation, and label in L with 1, 2 and 3 respectively the three connected components met during this trip (Figure (5b)).

(b) For each l = 1, 2, 3 (Figure (5c), (5d), (5e)), label with l all pixels in L which:

i. have the label 0, ii. are connected with an l labeled pixel ,iii. correspond to 1 valued pixels in the thinned ridge map.

(c) Count the number of 0 to 1, 0 to 2 and 0 to 3 transitions met when making a full clockwise trip along the border of the L image. The above three numbers are denoted by T_{01}, T_{02}, T_{01} respectively as shown in Figure (5f).

(d) If $T_{01} = 1$ & $T_{02} = 1$ & $T_{03} = 1$, then validate the candidate minutia as a true ridge bifurcation.

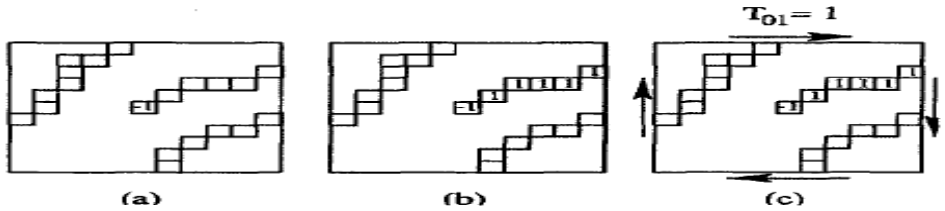

Figure 4: Steps to Validate Ridge Ending

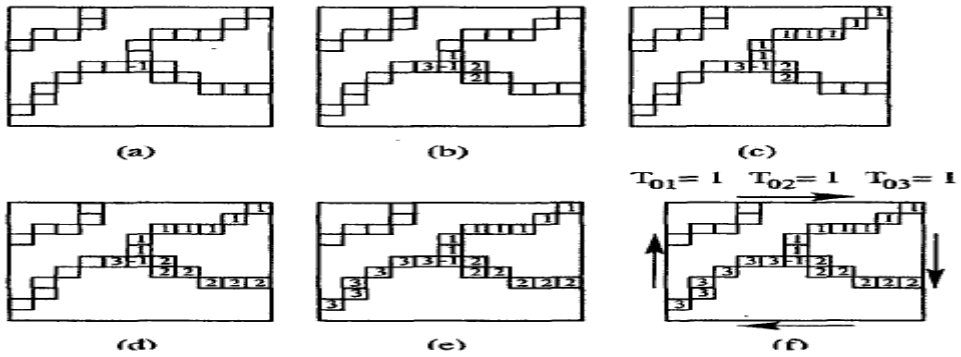

Figure 5: Steps to Validate Ridge Bifurcation

The dimension W of the neighborhood analyzed around each candidate minutia is chosen larger than two times the average distance between two neighborhood ridges. By this minutiae belonging to the same ridge are canceled.

3.3 Removal of False Minutiae Using Plus Rule

There is existence of false minutiae at boundary of fingerprint even after the above method of false minutiae removal. Some of pixels in border of fingerprint is marked as ridge ending but they are not actual ridge ending. These false minutiae are removed using plus rule [6]. The rule creates a plus sign on each minutia. It works on each minutia, to find a white pixel (i.e. '1' value) across these lines. If a white pixel is not detected, in any line, the minutia is marked as boundary minutia and hence removed.

3.4 Removal of False Minutiae Based on Average Inter-Ridge Distance

False ridge breaks due to insufficient amount of ink & ridge cross connections due to over inking may occur. Also some of the pre-processing steps introduce some spurious minutia points in the image. So to keep the recognition system consistent these false minutiae need to be removed.

The inter ridge distance D which is the average distance between two neighboring ridges is considered. For this scan each row to calculate the inter ridge distance using the formula [7]:

$$Inter\ ridge\ distance = \frac{sum\ all\ pixels\ with\ value\ 1}{row\ length} \quad (28)$$

Finally an averaged value over all rows gives D.

1. If d(bifurcation, termination) < D & the 2 minutia are in the same ridge then remove both of them.

2. If d(bifurcation, bifurcation) < D & the 2 minutia are in the same ridge them remove both of them.

3. If d(termination, termination) < D & the 2 minutia are in the same ridge them remove both of them.

where $d(X, Y)$ is the distance between 2 minutia points.

IV. EXPERIMENTAL RESULTS

Database of fingerprint is collected using optical fingerprint sensor Secugen Hamster Plus. The size of the ingerprint image captured is pixels and the resolution is 500 DPI. Fingerprint image captured is in bitmap format (gray image). Fingerprints of right hand forefinger are collected from 10 persons and from each person 20 fingerprints of same finger are collected.

Figure (6) is input fingerprint image captured using an optical fingerprint sensor. It has varied range of gray levels which is reduced using normalization, Figure (7) is the normalized image of input fingerprint, in which gray level variations are low in fingerprint ridges. Next is to separate fingerprint from the background. Figure (8) shows the segmentation mask where black region indicated the background and white region indicates fingerprint, Figure (9) is segmented normalized image obtained using segmentation mask on normalized image. Figure (10) is enhanced image obtained by gabor filtering the segmented normalized image using orientation and frequency. Figure (11) is inverse binarized image of enhanced image. Figure (12) is the thinnied image obtained by applying morphological operation on binarized image. The size of ridge is reduced to 1 pixel. Figure (13) is the minutiae marked image obtained using cross number method. Here, green circles indicates ridge endings and red circle indicates ridge bifurcation. In this lot of false minutiae points are present.In Figure (14) and Figure (16) false minutiae present over the fingerprint is removed leaving valid minutiae using average inter-ridge distance based method. In Figure (15) and Figure (17) false minutiae present over the fingerprint is removed leaving valid minutiae using connected component labeling method. we can see that lot of valid minutiae are detected and lot of false minutiae are retained using average inter-ridge distance based method. But almost all valid minutiae are detected with very few false minutiae using connected componet labeling approach.

Figure 6:Input Image

Figure 7: Normalised Image

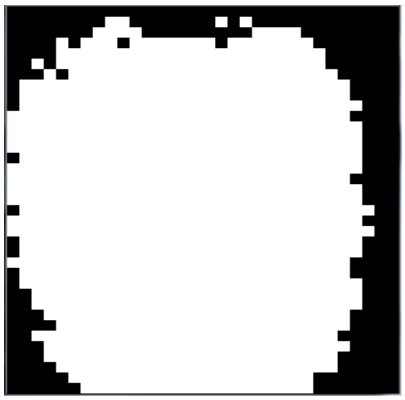

Figure 8: Segmentation Mask

Figure 9: Segmented Normalised Image

Figure 10: Enhanced Image

Figure 11: Binarised Image

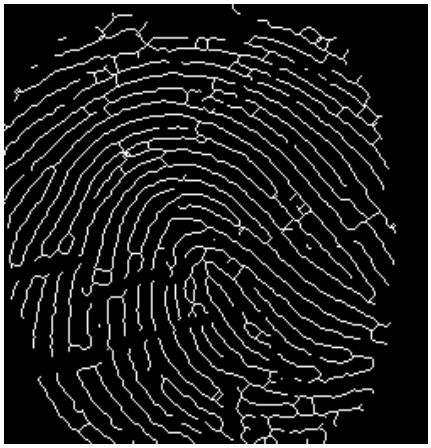

Figure 12: Thinned Image

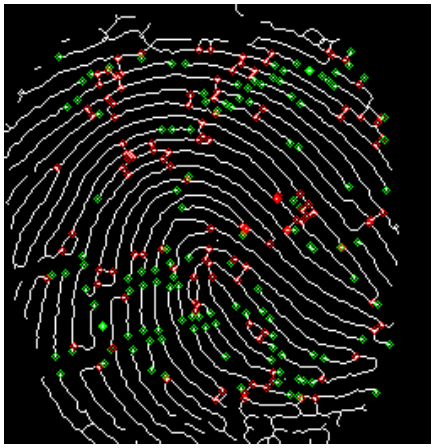

Figure 13: Minutiae Marked Image

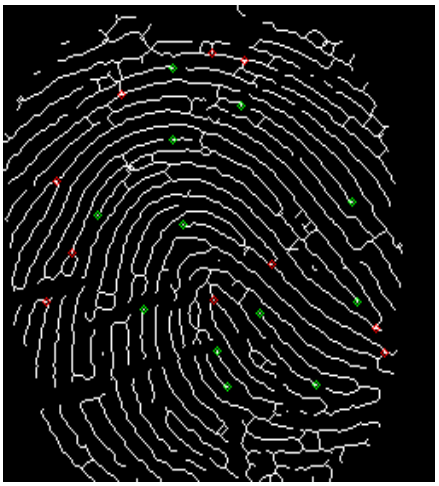

Figure 14: Valid Minutiae Using Average Connected Component inter-ridge distance Method

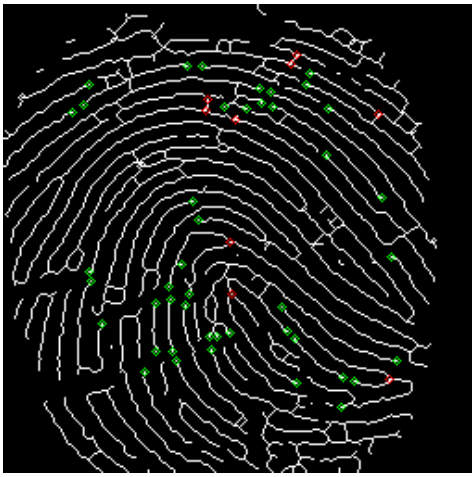

Figure 15: Valid minutiae using labeling method

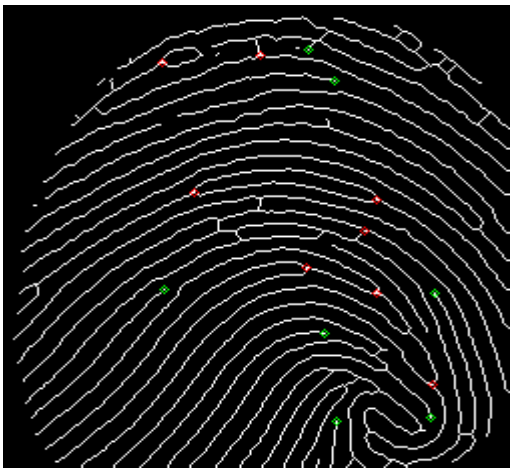

Figure 16: Valid minutiae using average connected component inter-ridge distance method

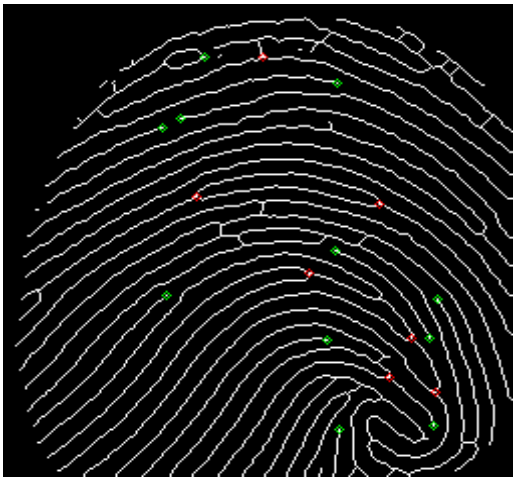

Figure 17: Valid minutiae using labeling method

V. CONCLUSION

The pre-processing, minutiae marking of fingerprint image is implemented. Also the two approaches for false minutiae removal is implemented and their performance is compared. Results obtained show that fingerprint image is enhanced better after pre-processing. Performance of removal of false minutiae is better using connected component labeling approach when compared to average inter-ridge distance based approach. It retains most valid minutiae with very few false minutiae. Enhancement of fingerprint image avoids existence of some false minutiae. But still some false minutiae will occur even after enhancement is removed by false minutiae removal methods. Using best method for false minutiae removal accuracy of fingerprint authentiaction system can be increased. i.e.false acceptance rate and false rejection rate can be achieved low.

REFERENCES

[1] Lin Hong, Yifei Wan, and Anil Jain,"Fingerprint Image Enhancement: Algorithm and Performance Evaluation", IEEE Transactions on Pattern Analysis And Machine Intelligence, Vol. 20, No. 8, August 1998.

[2] Ishmael S. Msiza, Mmamolatelo E. Mathekga, Fulufhelo V. Nelwamondo and Tshilidzi Marwala2," Fingerprint Segmentation: An Investigation Of Various Techniques And A Parameter Study Of A Variance-Based Method", International Journal of Innovative Computing, Information and Control, Volume 7, Number 9, September 2011.

[3] Z. Guo and R. Hall, "Parallel thinning with two-subiteration algorithms," Communications of the ACM, vol. 32, pp. 359–373, Mar 1989.

[4] Manvjeet Kaur, Mukhwinder Singh, Akshay Girdhar, and Parvinder S. Sandhu," Fingerprint Verification System using Minutiae Extraction Technique, World Academy of Science, Engineering and Technology,Vol:2, Oct 2008.

[5] Marius Tico, Pauli Kuosmanen, "An Algorithm for Fingerprint Image Post processing", IEEE Conference Record of the Thirty-Fourth Asilomar Conference on Signals, Systems and Computers, pp. 1735 1739, vol.2, Nov 2000.

[6] Shahida Jabeen, Shoab A. Khan, "A Hybrid False Minutiae Removal Algorithm with Boundary Elimination", IEEE International Conference on System of Systems Engineering, pp. 1-6, June 2008.

[7] Sachin Harne, K. J. Satao ," Minutiae Fingerprint Recognition Using Hausdorff Distance ",UNIASCIT, Vol 1 (1), pp. 16-22, 2011.

WIRELESS CHARGING

Sumit Dhangar[1], Ajinkya Korane[2]

[1,2] *UG, Mechanical Enggneering, Sandip Foundation (India)*

ABSTRACT

Mobile phones becoming a basic part of life, the recharging of mobile phone batteries have always been a problem. The mobile phones vary in their talk time and battery standby according to theirmanufacturer and batteries. All these phonesirrespective of their manufacturer andbatteries have to be put to recharge after thebattery has drained out. In this research, an innovative design of a wireless battery charger for portable electronic devices is proposed. The wireless power transfer is implemented through the magnetic coupling between a power transmitter, which is connected to the grid, and a power receiver, which is integrated inside the load device. An innovative receiver architecture which heavily improves the power conversion efficiency is presented. A laboratory prototype of the proposed wireless battery charger has been realized and tested to evaluate system performances. over the entire range of operating conditions the receiver efficiency lies within the 96.5% to99.9% range.

Keyword: Coupling, Prototype, Implemented, Portable, Wireless

I. INTRODUCTION

Wireless transfer has been employed since long time in telecommunications. Radio waves, cellular transmissions and Internet WiFi are only a few examples of wireless transmission. Recently, there's been a growing interest towards the experimentation of a deeply challenging idea for wireless applications: supplying electronic devices without cords. The development, application and spread of this new concept could make consumers life enormously easier, since wired chargers are often perceived as annoying and bulky objects. By magnetic induction , power transmitter is represented by a gridconnected magnetic pad while the power receiver is integrated inside the load device. Users should only place their portable device upon the magnetic pad. Magnetic coupling allows several devices to be simultaneously charged. In order to spread wireless battery charging, compatibility between chargers and devices is a key issue to deal with. Recently the Wireless Power Consortium (WPC) has built an international standard, also known as "Qi-standard", which aims at promoting the complete interoperability between power charging stations and rechargeable devices.

II. SHORT DISTANCE INDUCTION

These methods can reach at most a few centimeters. The action of an electrical transformer is the simplest instance of wireless energy transfer. The primary and secondary circuits of a transformer are electrically isolated from each other. The transfer of energy takes place by electromagnetic coupling through a process known as mutual induction. (An added benefit is the capability to step the primary voltage either up or down.) The electric toothbrush charger is an example of how this principle can be used.

III. WIRELESS POWER TRANSMISSION

A toothbrush's daily exposure to water makes a traditional plug-in charger potentially dangerous. Ordinary electrical connections could also allow water to seep into the toothbrush, damaging its components. Because of this, most toothbrushes recharge through inductive coupling. You can use the same principle to recharge several devices at once. For example, the Splashpower recharging mat and Edison Electric's Power desk both use coils to create a magnetic field. Electronic devices use corresponding built-in or plug-in receivers to recharge while resting on the mat. These receivers contain compatible coils and the circuitry necessary to deliver electricity to devices' batteries

IV. MODERATE DISTANCE

Resonance and Wireless Power Household devices produce relatively small magnetic fields. For this reason, chargers hold devices at the distance necessary to induce a current, which can only happen if the coils are close together. A larger, stronger field could induce current from farther away, but the process would be extremely inefficient. Since a magnetic field spreads in all directions, making a larger one would waste a lot of energy. An efficient way to transfer power between coils separated by a few meters is that we could extend the distance between the coils by adding resonance to the equation. A good way to understand resonance is to think of it in terms of sound. An object's physical structure -- like the size and shape of a trumpet -- determines the frequency at which it naturally vibrates. This is its resonant frequency. It's easy to get objects to vibrate at their resonant frequency and difficult to get them to vibrate at other frequencies. This is why playing a trumpet can cause a nearby trumpet to begin to vibrate. Both trumpets have the same resonant frequency. Induction can take place a little differently if the electromagnetic fields around the coils resonate at the same frequency. The theory uses a curved coil of wire as an inductor. A capacitance plate, which can hold a charge, attaches to each end of the coil. As electricity travels through this coil, the coil begins to resonate. Its resonant frequency is a product of the inductance of the coil and the capacitance of the plates.

V. THE WIRELESS POWER FROM CURVED COIL AND CAPACITIVE PLATES

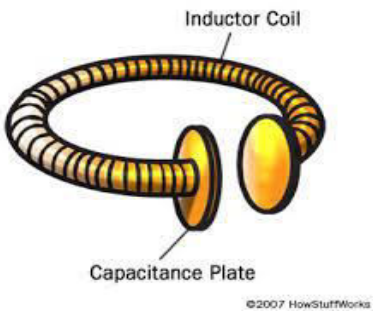

Electricity, traveling along an electromagnetic wave, can tunnel from one coil to the other as long as they both have the same resonant frequency. In a short theoretical analysis they demonstrate that by sending electromagnetic waves around in a highly angular waveguide, evanescent waves are produced which carry no energy. An evanscent wave is nearfield standing wave exhibiting exponential decay with distance. If a proper resonant waveguide is brought near the transmitter, the evanescent waves can allow the energy to tunnel (specifically evanescent wave coupling, the electromagnetic equivalent of tunneling to the power drawing waveguide, where they can be rectified into DC power. Since the electromagnetic waves would tunnel, they would not propagate through the air to be absorbed or dissipated, and would not disrupt electronic devices. As long as both coils are out of range of one another, nothing will happen, since the fields around the coils aren't strong enough to affect much around them. Similarly, if the two coils resonate at different frequencies, nothing will happen. But if two resonating coils with the same frequency get within a few meters of each other, streams of energy move from the transmitting coil to the receiving coil. According to the theory, one coil can even send electricity to several receiving coils, as long as they all resonate at the same frequency. The researchers have named this non-radiative energy transfer since it involves stationary fields around the coils rather than fields that spread in all directions.

VI. WIRELESS POWER TRANSMISSION

According to the theory, one coil can recharge any device that is in range, as long as the coils have the same resonant frequency. "Resonant inductive coupling" has key implications in solving the two main problems associated with non-resonant inductive coupling and electromagnetic radiation, one of which is caused by the other; distance and efficiency. Electromagnetic induction works on the principle of a primary coil generating a predominantly magnetic field and a secondary coil being within that field so a current is induced within its coils. This causes the relatively short range due to the amount of power required to produce an electromagnetic field. Over greater distances the non-resonant induction method is inefficient and wastes much of the transmitted energy just to increase range. This is where the resonance comes in and helps efficiency dramatically by "tunneling" the magnetic field to a receiver
coil that resonates at the same frequency. Unlike the multiple-layer secondary of a non-resonant transformer, such receiving coils are single layer solenoids with closely spaced capacitor plates on each end, which in combination allow the coil to be tuned to the transmitter frequency thereby eliminating the wide energy wasting "wave problem" and allowing the energy used to focus in on a specific frequency increasing the range.

VII. LONG-DISTANCE WIRELESS POWER

Whether or not it incorporates resonance, induction generally sends power over relatively short distances. But some plans for wireless power involve moving electricity over a span of miles. A few proposals even involve sending power to the Earth from space. In the 1980s, Canada's Communications Research Centre created a small airplane that could run off power beamed from the Earth. The unmanned plane, called the Stationary High Altitude Relay Platform (SHARP), was designed as a communications relay. Rather flying from point to point, the SHARP could fly in circles two kilometers in diameter at an altitude of about 13 miles (21 kilometers). Most importantly, the aircraft could fly for months at a time.

The secret to the SHARP's long flight time was a large, ground-based microwave transmitter. The SHARP's circular flight path kept it in range of this transmitter. A large, disc-shaped rectifying antenna, or rectenna, just behind the plane's wings changed the microwave energy from the transmitter into direct-current (DC) electricity. Because of the microwaves' interaction with the rectenna, the SHARP had a constant power supply as long as it was in range of a functioning microwave array. Rectifying antennae are central to many wireless power transmission theories. They are usually made an array of dipole antennae, which have positive and negative poles. These antennae connect to shottkey diodes. Here's what happens:

1. Microwaves, which are part of the electromagnetic spectrum reach the dipole antennae. 2. The antennae collect the microwave energy and transmit it to the diodes. 3. The diodes act like switches that are open or closed as well as turnstiles that let electrons flow in only one direction. They direct the electrons to the rectenna's circuitry. 4. The circuitry routes the electrons to the parts and systems that need them.
2. Wireless Charging Techniques Three major techniques for wireless charging are magnetic inductive coupling, magnetic resonance coupling, and microwave radiation. The magnetic inductive and magnetic resonance coupling work on near field, where the generated electromagnetic field dominates the region close to the transmitter or 3 (a) Inductive Coupling (b) Magnetic Resonance Coupling (c) Far-field Wireless Charging scattering object. The near-field power is attenuated according to the cube of the reciprocal of the distance. Alternatively, the microwave radiation works on far field at a greater distance. The far-field power decreases according to the reciprocal of the distance. Moreover, for the far-field technique , the absorption of radiation does not affect the transmitter. By contrast, for the near-field techniques, the absorption of radiation influences the load on the transmitter. 1) Magnetic Inductive Coupling: Magnetic inductive coupling is based on magnetic field induction that delivers electrical energy between two coils. Magnetic inductive coupling happens when a primary coil of an energy transmitter generates predominant varying magnetic field across the secondary coil of the energy receiver within the field, generally less than the wavelength. The near-field power then induces voltage/current across the secondary coil of the energy receiver within the field. This voltage can be used by a wireless device. The energy efficiency depends on the tightness of coupling between two coils and their quality factor. The tightness of coupling is determined by the alignment and distance, the ratio of diameters, and the shape of two coils. The quality factor mainly depends on the materials, given the shape and size of the coils as well as the operating frequency. The advantages of magnetic inductive coupling include ease of implementation, convenient operation, high efficiency in close distance (typically less than a coil diameter) and safety. Therefore, it is applicable 4 and popular for mobile devices. Very recently, MIT scientists have announced the invention of a novel wireless charging technology, called MagMIMO, which manages to charge a wireless device from up to 30 centimeters away. It is claimed that MagMIMO can detect and cast a cone of energy towards a phone, even when the phone is put inside the pocket. 2) Magnetic Resonant Coupling: Magnetic resonance coupling .As the resonant coils, operating at the same resonant frequency, are strongly coupled, high energy transfer efficiency can be achieved with small leakage to non-resonant externalities. This property also provides the advantage of immunity to neighboring environment and line-of-sight transfer requirement. Compared to magnetic inductive coupling, another advantage of magnetic resonance charging is longer effective charging distance. Additionally, magnetic resonant coupling can be applied between one transmitting resonator and many receiving resonators, which enables concurrent charging of multiple devices. In 2007, MIT scientists proposed a high-efficient mid-range wireless power transfer technology, i.e., Witricity, based on strongly coupled magnetic resonance. It was reported that wireless power

transmission can light a 60W bulb in more than two meters with transmission efficiency around 40% [6]. The efficiency increased up to 90% when the transmission distance is one meter. However, it is difficult to reduce the size of a Witricity receiver because it requires a distributed capacitive of coil to operate. This poses big challenge in implementing Witricity technology in portable devices. Resonant magnetic coupling can charge multiple devices concurrently by tuning coupled resonators of multiple receiving coils. This has been shown to achieve improved overall efficiency. However, mutual coupling of receiving coils can result in interference, and thus proper tuning is required. 3) Microwave Radiation: Microwave radiation utilizes microwave as a medium to carry radiant energy. Microwaves propagate over space at the speed of light, normally in line-of-sight. Figure 1c shows the architecture of a microwave power transmission system. The power transmission starts with the ACto-DC conversion, followed by a DC-to-RF conversion through magnetron at the transmitter side. After propagated through the air, the microwaves captured by the receiver rectenna are rectified into electricity again. The typical frequency of microwaves ranges from 300MHz to 300GHz. The energy transfer can use other electromagnetic waves such as infrared and X-rays. However, due to safety issue, they are not widely used. The microwave energy can be radiated isotropically or towards some direction through beamforming. 5 The former is more suitable for broadcast applications. For point-to-point transmission, beamforming transmit electromagnetic waves, referred to as power beamforming, can improve the power transmission efficiency. A beam can be generated through an antenna array (or aperture antenna). The sharpness of power beamforming improves with the number of transmit antennas. The use of massive antenna arrays can increase the sharpness. The recent development has also brought commercial products into the market. For example, the Powercaster transmitter and Powerharvester receiver allow 1W or 3W isotropic wireless power transfer. Besides longer transmission distance, microwave radiation offers the advantage of compatibility with existing communication system. Microwaves have been advocated to deliver energy and transfer information at the same time. The amplitude and phase of microwave are used to modulate information, while the radiation and vibration of microwaves are used to carry energy. This concept is referred to as simultaneous wireless information and power transfer (SWIPT). However, due to health concern of RF radiations, the power beacons are constrained by the Federal Communications Commission (FCC) regulation, which allows up to 4 watts for effective isotropic radiated power, i.e., 1 watt device output power plus 6dBi of antenna gain. Therefore, dense deployment of power beacons is required to power hand-held cellular mobiles with lower power and shorter distance. The microwave energy harvesting efficiency is significantly dependent on the power density at receive antenna.

Table 1: Comparison Between Different Wireless Charging Techniques

Wireless charging technique	Advantage	Disadvantage	Effective charging distance	Applications
Inductive coupling	Safe for human, simple implementation	Short charging distance, heating effect, Not suitable for mobile	From a few millimeters to a few centimeter	Mobile electronics (e.g, smart phones and tablets), toothbrush,

		applications, needs tight alignment between chargers and charging devices		RFID tags, contactless smart cards
Magnetic resonance coupling	Loose alignment between chargers and charging devices, charging multiple devices simultaneously on different power,	Not suitable for mobile applications, Limited charging distance, Complex implemental	From a few centimeters to a few meters	Mobile electronics, home appliances (e.g., TV and desktop), electric vehicle charging
Microwave radiation	Long effective charging distance, Suitable for mobile applications	Not safe when the RF density exposure is high, Low charging efficiency	Typically within several tens of meters, up to several kilometers	RFID cards, wireless sensors, implanted body devices, LEDs

VIII. CIRCUIT DIAGRAM

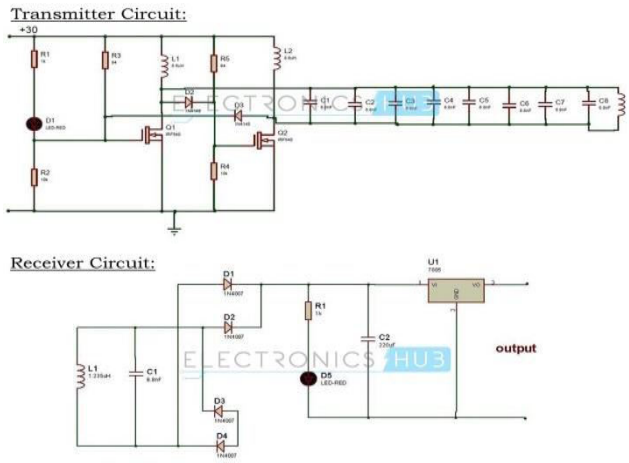

Figure 1: Transmitter and Receiver Circuit

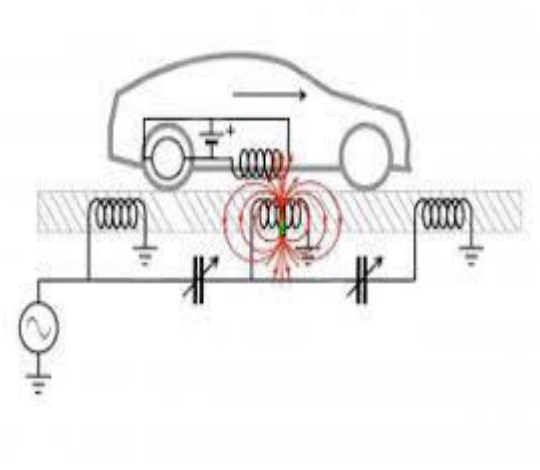

Figure2: Resonance Concept of Charging

IX. CONCLUSION

In conclusion, it is clear that resonant inductive coupling power transmission would be extremely beneficial to society if it were implemented in homes and home electronics. From an environmental standpoint, this technology could replace disposable batteries and cords, reducing dangerous chemicals and potential for poisoning communities. Resonant inductive coupling also has health benefits and with no need for cords life

would simply become easier. With the help of this technology As long as the device is in a room equipped with a source of such wireless power, it would charge

Automatically, without having to be plugged in. In fact, it would not even need a battery to operate inside of such a room." In the long run, this could reduce our society's dependence on batteries, which are currently heavy and expensive. At the same time for the long range power transmission, power can be sent from source to receivers instantaneously without wires, reducing the cost.

Thus by inductive coupling technique there will be reduction per unit cost of power transmission.

ANALYSIS OF ANTI-OXIDANT AND ANTI-AGEING PROPERTIES OF ALOE VERA GEL ON LIFE HISTORY PARAMETERS OF DROSOPHILA MELANOGASTER

Usha Mathur[1], Manvender Singh Gahlout[2], Nisha[3], Veer Bhan[4]

[1]PG Student, [2]Associate Professor, [3]PG Student, [4]Assistant Professor, Department of Biotechnology, University Institute of Engineering & Technology, Maharshi Dayanand University, Rohtak (India)

ABSTRACT

If aging is due to or contributed by free radical reactions, as postulated by the free radical theory of aging, lifespan of organisms should be extended by administration of exogenous antioxidants In the present study, we tested the effect of larval diet supplementation with five different concentrations of Aloe vera gel on the adult longevity of short-lived D melanogaster populations. A vera gel supplementation of larval diet extended adult longevity in both the male and female flies without reducing fecundity but by efficient reactive oxygen species scavenging through increased antioxidant enzymes activity and better neuroprotection as indicated by increased locomotor activity in adult males.

Keywords: Anti-Oxidant, Drosophila Melanogaster, Fecundity, Longevity, SOD.

I. INTRODUCTION

Aging generally refers to the process of getting chronologically older and it is typically accompanied by senescence, the gradual loss of physiological functions. Both of these processes are to some degree, inevitable for all living organisms. Chronological aging is primarily predetermined by heredity, whereas senescence results from a complex interaction between environmental and genetic factors. Non-genetic factors such as nutrition, environmental quality, psychosocial factors, and lifestyle play an important role in healthy aging.

It is well known that Reactive Oxygen Species (ROS) have been implicated in more than 100 diseases, including malaria, acquired immune deficiency syndrome, heart disease, stroke, arteriosclerosis, diabetes and cancer (Tanizawa *et al*., 1992; Alho and Leinonen, 1999). In *Drosophila*, a single locus, *Sod*, encodes the cytosolic enzyme Cu/Zn superoxide dismutase (CuZnSOD), which is an essential component in a major antioxidant defense pathway for scavenging reactive oxygen species (ROS) generated during aerobic respiration (Seto *et al.,* 1989; Noor *et al.,* 2002). Nevertheless, all aerobic organisms, including human beings, have antioxidant defenses that protect against oxidative damages. However, this natural antioxidant mechanism can be inefficient; hence, dietary intake of antioxidant compounds becomes important (Halliwell, 1994; Terao *et al*., 1994). Therefore, research for the determination of source of the natural antioxidants is important.

Therefore, research for the determination of source of the natural antioxidants is important. Recently there has been an upsurge of interest in the therapeutic potentials of plants, as antioxidants in reducing free radical

induced tissue injury. Medicinal plants are considered to be the best source for antioxidant compounds. As plants produce significant amount of antioxidants to prevent the oxidative stress caused by photons and oxygen, they are considered as potential source of antioxidant compounds. India is perhaps the largest producer of medicinal herbs and is rightly called the "Botanical garden of the World".

Aloe vera is the oldest medicinal plant ever known and the most applied medicinal plant worldwide. Aloe vera is a succulent plant species that is found only in cultivation, having no naturally occurring populations, although closely related aloes do occur in northern Africa (Akinyele 2007) The common names of Aloe vera are Aloe vera, Aloe, burn plant, lily of the desert, elephant's gall and Latin name is Aloe barbadensis The species is frequently cited as being used in herbal_medicine since the beginning of the first century AD. Extracts from A. vera are widely used in the cosmetics and alternative medicine industries, being marketed as variously having rejuvenating, healing, or soothing properties. There is, however, little scientific evidence of the effectiveness or safety of Aloe vera extracts for either cosmetic or medicinal purposes, and what positive evidence is available is frequently contradicted by other studies (Ernst E 2000, Marshall JM 1990, Boudreau MD, Beland FA 2006, Vogler BK, Ernst E Oct 1999).

Fruit fly is one of the models to study aging and age-related diseases (Jafari, 2010). Humans actually share a huge amount of conserved biological pathways and diseases-causing genes with this tiny insect (Reiter et al., 2001; Bauer et al., 2004). Compared with other models, fruit fly is relatively easier to maintain in a large quantity due to their tiny body size and short lifespan. Previous reports have revealed that dietary modification, including calorie restriction and dietary supplementation, can extend lifespan and ameliorate certain age-related diseases (McCay et al., 1935; Lin et al., 2002; Partridge et al., 2005; Lee et al., 2006; Piper and Bartke, 2008).

In the present study, we analyzed the effect of ageing on the antioxidant enzyme system and compared with flies supplemented with Aloe vera gel. SOD activity was found to unregulated in *A vera* gel fed flies as compared to that of flies fed on standard *Drosophila food medium*. Protein content found increased in Aloe vera gel fed flies as compare to control flies. Our results suggest that supplementation with Aloe vera gel reduces oxidative stress and improves longevity.

II. MATERIAL AND METHODS

2.1 Fly Strains and Diet

Wild type strain of *Drosophila* was used in the present study. The flies were cultured on *Drosophila* food medium containing agar-agar, corn meal, sugar, yeast, anti-bacterial, anti-fungal agent at 21 ºC±1. The additional yeast suspensions were provided for healthy growth. Four experimental diets were prepared by adding Aloe vera gel at 3 ml, 5 ml, 7ml and 10ml in the control diet per liter.

2.2 Effect of Aloe vera gel on longevity and fecundity of Drosophila flies fed the basal diet

Two independent trials were conducted. For each trial, newly eclosed male flies were divided into 5 groups (n=200 each), and housed in 10 vials (20 flies per vial). The first group was maintained on the basal diet, while the other experimental group was fed one of the Aloe vera gel diet. Dead flies were counted every 2–3 days and the remaining alive flies were transferred to a new vial containing the same diet. The maximum life spans in this study were calculated as the average life span of the 5% longest surviving flies. The same experiments described above were similarly repeated and the fruit flies were sacrificed in order to quantify the expression of SOD, and protein content.

2.3. Climbing Assay

Climbing ability of fruit flies was assessed using the climbing assay. In this assay 10 male flies were placed in a plastic vial, given 10 s to climb up. At the end of each trial, the number of flies that climbed up to a vertical distance of 8 cm or above was recorded. Each trial was performed three times.

2.4 Statistical Analyses

In all cases except survival function analysis, the population means were used as the units of analysis. The significance of the difference between means was assessed using one-way analysis of variance. The differences among treatments were compared by Tukey–Kramer Minimum Significant Difference. The significance of the difference between adult survival curves was analyzed using Kaplan–Meier log-rank test.

III. RESULTS

3.1 Longevity and Fecundity

Supplementation of diet with *A vera* significantly changed the average longevity of female flies ($F7,16 = 5.4159$, $p = .005$) but not of male flies ($F7,16 = 2.984$, $p = .10$). The median life span of both female and male flies was not significantly altered by diet supplementation. However, the maximum life span was significantly altered in both the sexes (Table 1). The increase in longevity of female flies was not linked to loss of fertility as there was no significant effect of diet supplementation with *A vera* on lifetime fecundity ($F7,16 = 2.0296$, $p = .114$). The survival rates of both female and male flies were significantly affected by *A vera* supplementation.

Table 1: Data on mean values of Fecundity, Percent viability and longevity of male and female individuals of Drosophila melanogaster fed on Control and Aloe vera gel supplemented food medium.

Treatment groups	Fecundity	Percent Viability	Longevity (Days)	
			Male	Female
Control	171	91.13	50	56
A vera (3ml/lt)	180	91.2	57	70
A vera (5ml/lt)	187	93.8	61	75
A vera (7ml/lt)	195	96	63	78
A vera (10ml/lt)	197	97.3	65	80

3.2 Superoxide Dismutase Activity

Superoxide dismutase activity was significantly upregulated in male ($F7,16 = 66.4002$, $p = .000$) and female ($F7,16 = 18.9459$, $p = .000$) flies by *A vera* supplementation.

3.3 Climbing Activity

Male climbing activity was significantly influenced by diet supplementation with *A vera* ($F7,16 = 138.7598$, $p = .000$). Flies reared on 10ml/litre of A vera gel were the most active, whereas the standard control flies were the least active (Table 2).

Table 2: Data on mean values of chill coma recovery and climbing assyay of Drosophila melanogaster fed on Control and Aloe vera gel supplemented food medium.

Treatment groups	Climbing Time	
	Male	Female
Control	11.3	8.4
A vera (3ml/lt)	9.5	7.5
A vera (5ml/lt)	7.2	6.3
A vera (7ml/lt)	6	5.4
A vera (10ml/lt)	5	4.3

IV. DISCUSSION

In the present study, anti-oxidant and anti-ageing effects of Aloe vera gel were analyzed on the life history parameters of D. melanogaster. Aloe vera gel could prolong the mean lifespan of fruit flies by >10% compared with the control. The present study also demonstrated that supplementation of aloe vera gel was associated with elevated mRNA level of SOD at Drosophila. The increased locomotor activity of flies reared on media supplemented with resveratrol could have been due to its neuroprotective activity (Mokni M, Elkahoui S, Limam F, et al. 2007; Araki T, Sasaki Y, Milbrandt J. 2004; Parker JA, Arango M, Abderrahmane S, et al. 2005; Wang Q, Xu J, Rottinghaus GE, et al. 2002; Wang Q, Yu S, Simonyi A, et al. 2004; Han YS, Zheng WH, Bastianetto S, et al. 2004). In another study, feeding fish with resveratrol-supplemented diet prevented age-dependent neurodegeneration (Valenzano DR, Terzibasi E, Genade T, et al. 2006). In addition to neuroprotection, resveratrol could have stimulated the growth and regeneration of nerve fibers that could have resulted in increased preadult viability, because the larval growing media was modified in this study, unlike all other studies that altered the adult diet. The lipid content of the flies raised as larvae on *A vera* extract–supplemented diet suggests that *A vera* extends longevity through mechanisms other than calorie restriction, as increased longevity in dietary restriction studies were associated with increased lipid content and reduced dry weight and fecundity (Simmons FH, Bradley TJ. 1997). Longevity extension by *A vera* is probably mediated through prevention of neurodegeneration and/or regeneration of nerve fibers as indicated by increased locomotor activity. Increased activity of detoxifying enzymes SOD and catalase seems to be able to clear the system of the toxic elements that could have otherwise caused damage and lead to no improvement in longevity.

Aloe vera is known to contain a plethora of phytochemicals, such as 1,8-dihydroxyanthraquinone derivatives and their glycosides, proteins, lipids, amino acids, vitamins, enzymes, inorganic compounds, and small organic compounds (Hamman JH. 2008), some, if not most of them could have contributed to improved health through correction of many metabolic processes—anthraquinone is a starting material for production of antioxidants to cite one example. *Aloe vera* extract seems to mimic the longevity extension effects of resveratrol as well as morphine (Dubiley TA, Rushkevich YE, Koshel NM, et al. 2011) through regeneration of nerve fibers, neuroprotection as indicated by increased locomotor activity, and upregulation of detoxifying enzymes.

REFERENCES

[1]. Akinyele BO, Odiyi AC (2007). "Comparative study of the vegetative morphology and the existing taxonomic status of Aloe vera L.". Journal of Plant Sciences 2 (5): 558–563.

[2]. Alho, H. and J. Leinonen (1999). Total antioxidant activity measured by chemiluminescence method. Methods Enzymol., 299: 3-15.

[3]. Araki T, Sasaki Y, Milbrandt J. Increased nuclear NAD biosynthesis and SIRT1 activation prevent axonal degeneration. Science. 2004;305:1010–1013.

[4]. Bauer, J.H., Goupil, S., Garber, G.B., Helfand, S.L., 2004. An accelerated assay for the identification of lifespan-extending interventions in Drosophila melanogaster. Proc. Natl. Acad. Sci. U. S. A. 101, 12980–12985.

[5]. Boudreau MD, Beland FA (2006). "An Evaluation of the Biological and Toxicological Properties of Aloe Barbadensis (Miller), Aloe Vera". Journal of Environmental Science and Health Part C 24: 103–154.

[6]. Dubiley TA, Rushkevich YE, Koshel NM, et al. Life span extension in Drosophila melanogaster induced by morphine. Biogerontology. 2011;12:179–184.

[7]. Ernst E (2000). "Adverse effects of herbal drugs in dermatology". Br J Dermatol 143(5): 923–929.

[8]. Halliwell, B. (1994). Free radicals antioxidants and human disease: Curiosity, cause or consequence. Lanset, 344: 721-724.

[9]. Hamman JH. Composition and applications of Aloe vera leaf gel. Molecules. 2008;13:1599–1616.

[10]. Han YS, Zheng WH, Bastianetto S, et al. Neuroprotective effects of resveratrol against beta-amyloid-induced neurotoxicity in rat hippocampal neurons: involvement of protein kinase C. Br J Pharmacol. 2004;141:997–1005.

[11]. Jafari, M., 2010. Drosophila melanogaster as a model system for the evaluation of antiaging compounds. Fly (Austin) 4 .

[12]. Lee, G.D., Wilson, M.A., Zhu, M., Wolkow, C.A., de Cabo, R., Ingram, D.K., Zou, S., 2006. Dietary deprivation extends lifespan in Caenorhabditis elegans. Aging Cell 5, 515–524.

[13]. Lin, S.J., Kaeberlein, M., Andalis, A.A., Sturtz, L.A., Defossez, P.A., Culotta, V.C., Fink, G.R., Guarente, L., 2002. Calorie restriction extends Saccharomyces cerevisiae lifespan by increasing respiration. Nature 418, 344–348.

[14]. Marshall JM (1990). "Aloe vera gel: what is the evidence?". Pharm J 244: 360–362.

[15]. McCay, C.M., Crowell, M.F., Maynard, L.A., 1935. The effect of retarded growth upon the length of life and upon the ultimate body size. J. Nutr. 10, 63–79.

[16]. Mokni M, Elkahoui S, Limam F, et al. Effect of resveratrol on antioxidant enzyme activities in the brain of healthy rat. Neurochem Res. 2007;32:981–987.

[17]. Noor R, Mittal S, Iqbal J (2002) Superoxide dismutase: Applications and relevance to human diseases. Med Sci Monit 8:RA210–RA215.

[18]. Parker JA, Arango M, Abderrahmane S, et al. Resveratrol rescues mutant polyglutamine cytotoxicity in nematode and mammalian neurons. Nat Genet. 2005;37:349–350.

[19]. Partridge, L., Piper, M.D., Mair, W., 2005. Dietary restriction in Drosophila. Mech. Aging Dev. 126, 938–950.

[20]. Piper, M.D., Bartke, A., 2008. Diet and aging. Cell Metab. 8, 99–104.

[21]. Reiter, L.T., Potocki, L., Chien, S., Gribskov, M., Bier, E., 2001. A systematic analysis of human disease-associated gene sequences in Drosophila melanogaster. Genome Res. 11, 1114–1125.

[22]. Seto NOL, Hayashi S, Tener GM (1989) Cloning, sequence analysis and chromosomal localization of the Cu-Zn superoxide dismutase gene of Drosophila melanogaster. Gene 75: 85–92.

[23]. Simmons FH, Bradley TJ. An analysis of resource allocation in response to dietary yeast in Drosophila melanogaster. J Insect Physiol. 1997;43:779–788.

[24]. Tanizawa, H., Y. Ohkawa, Y. Takino, A. Ueno, T. Kageyama and S. Hara (1992). Studies on natural antioxidants in Citrus species. I. Determination of antioxidant activity of citrus fruits. Chem. Pham. Bull., 40: 1940-1942.

[25]. Terao, J., M. Piskula and Q. Yao (1994). Protective effect of epicatechin, epicatechin gallate and quercetin on lipid peroxidation in phospholipid bilayers. Arch. Biochem. Biophys., 308: 278-284.

[26]. Valenzano DR, Terzibasi E, Genade T, et al. Resveratrol prolongs lifespan and retards the onset of age-related markers in a short lived vertebrate. Curr Biol. 2006;16:296–300.

[27]. Vogler BK, Ernst E (Oct 1999). "Aloe vera: a systematic review of its clinical effectiveness". Br J Gen Pract 49 (447): 823–8.

[28]. Wang Q, Xu J, Rottinghaus GE, et al. Resveratrol protects against global cerebral ischemic injury in gerbils. Brain Res. 2002;958:439–447.

[29]. Wang Q, Yu S, Simonyi A, et al. Resveratrol protects against neurotoxicity induced by kainic acid. Neurochem Res. 2004;29:2105–2112.

MICROSTRUCTURE AND MECHANICAL PROPERTIES OF AL6061-CENOSPHERE-TİN BASED MMC'S

G.J.Naveen[1], C.Siddaraju[2], L.H.Manjunatha[3]

[1]Researcher, Centre for Surface Engineering and Research, P.E.S Institute of Technology, Bengaluru, Karnataka, (India)

[2]Assistant Professor, Dept of ME, M.S.Ramaiah Institute of Technology, Bengaluru,Karnataka, (India)

[3]Professor and Head , Dept of ME,Reva Institute of Technology and Management, Bengaluru, Karnataka, (India)

ABSTRACT

During the last two decades, metal matrix composites (MMCs) have emerged as an important class of materials for structural, wear, thermal, transportation and electrical applications. Manufacturing of aluminum alloy based composite materials via stir casting is one of the prominent and economical route for development and processing of metal matrix composite materials and significantly casting is one of the oldest manufacturing processes amongst all. In the light of the above, present study reveals the microstructure characterization and mechanical properties of the samples obtained by the stir casting technique(vortex method).The tested samples are examined using Scanning Electron microscope (SEM) on the surface of composites. The results of the research work shows that the proposed composites are compared with Al based metal matrix composites at corresponding values of test parameters. Results reveal that, increased content of cenosphere particles in matrix alloy increases various mechanical properties upto an extent of cenosphere by 15% in volume fraction; when compared with base material. Technical difficulties in attaining a uniform distribution of reinforcement, good wettability and a low porosity material are keenly given priority. The experimental results indicate that aluminum matrix cast composite can be manufactured via conventional foundry method giving very good responses to the strength and ductility up to 15% by volume of cenosphere with 1%TiN reinforced particles.

Keywords:: Al6061, Cenosphere, MetalMatrixComposites,Microstructure, SEM, Stircasting,TiN.

I. INTRODUCTİON

Modern development in the field of science and technology demands the development of advanced engineering materials for various engineering applications; especially in the areas of transportation, aerospace and military engineering . Composite materials are heterogeneous mixture of two or more homogeneous phases, which have been bonded together. Composite materials are formed by combining two or more materials that have different properties. Aluminum is the most widely used matrix material, in the investigations involving metal matrix composites (MMCs). This is mainly because of the unique combination of its low density, high strength, good

mechanical properties, good corrosion resistance and good machinability properties. The different materials work together to give the composite unique properties. Conventional monolithic materials have limitations in achieving good combination of strength, stiffness, toughness and density. To meet the ever increasing demand of modern day technology, composites are most promising materials of recent interest. Metal composites possess significantly improved properties including high specific strength; specific modulus, damping capacity and good wear resistance compared to unreinforced alloys. Among various discontinuous dispersoids used, cenosphere is one of the most inexpensive and low density reinforcement available in large quantities as solid waste by-product during combustion of coal in thermal power plants. The process of burning coal in thermal power plants produces fly ash containing ceramic particles made largely of alumina and silica. The ceramic particles in fly ash have three types of structures. The first type of particle is solid and is called precipitator. The second type of particle is hollow and is called cenospheres. The third type of particle is called plerospheres, which are hollow particles of large diameter filled with smaller size precipitator and cenospheres. Due to the hollow structure cenospheres have low density. Hence, composites with cenosphere as one of the reinforcement are likely to overcome the cost barrier for wide range applications in automotive and aerospace. It is thereby expected that the incorporation of cenosphere particles in aluminium alloy will promote yet another use of these low-cost waste by-product and at the same time, has the potential for conserving energy intensive aluminium thereby; reducing the cost of aluminium products[1-6].

II. EXPERIMENTAL PROCEDURE

Al6061 alloy with the chemical composition given in Table 1 was used as the matrix material. The reinforcement particulates (Table 2 and Table 3) with chemical composition are Cenosphere obtained from Raichur Thermal Power Station, Karnataka and treated in CPRI, Bengaluru; TiN sample procured from Vipra Chemicals, Mumbai respectively.

Table.1 Chemical Composition of Al6061alloy

Elements	Si	Fe	Cu	Mn	Ni	Zn	Ti	Mg	Al
Percentage	0.43	0.43	0.24	0.13	<0.05	0.006	0.02	0.802	Bal

Table.2 Chemical Composition of Cenosphere

Elements	Si	Al	FeO	Ti
Percentage	0.65	0.3	0.03	0.02

Table.3 Chemical Composition of Titanium Nitride (Powder)

Elements	O	N	Fe	C	Cr	Mg	Al	Si
Percentage	0.98	0.22	0.13	0.02	0.04	0.02	0.004	<0.005

The synthesis of the composite was carried out by stir casting. The ingots of Aluminum 6061 alloy were taken in a graphite crucible and melted in an electric furnace. The temperature was slowly raised to 750°C. The melt was degassed at 700°C using a solid dry hexachloroethane (C_2Cl_6, 0.5 wt. %) degasser. The molten metal was stirred to create a vortex and the particulates were introduced. The degassed molten metal was placed below the stirrer and stirred at approximately 200 rpm and was maintained between 5 to 7 min. The preheated titanium nitride and cenosphere (fly ash) particles were slowly added into the melt. The percentage of cenosphere added was 5, 10, or 15 wt. % and titanium nitride was kept constant at 1% wt. The stirred dispersed molten metal was

poured into preheated S.G. iron mould 22 mm in diameter and 220 mm height. The pouring temperature was maintained at 680ºC.The melt was then allowed to solidify in the mould and cooled to room temperature. Below photographs show the various steps involved in stir casting (vortex method).

Electrical Melting Furnace

Melting (attaining molten state)

Impeller @ 200 rpm speed

Stirring the Mixture(Matrix + Reinforcement)

Formation of Slag

Removing the impurities – SLAG

Pouring the molten metal

III. RESULTS

Microstructural characterization studies were conducted to examine distribution of reinforcement throughout the matrix. This is accomplished by using scanning electron microscope. The composite samples were metallographically polished prior to examination. Characterization is done in etched conditions. Etching was accomplished using Keller's reagent. It is observed that cenosphere and TiN particles are fairly homogeneously distributed; evident from the SEM below and reinforced phase is also noticed in some composites with higher weight percentage of cenosphere particles. Further, there exists strong interfacial bond between matrix alloy and reinforcement as a beneficial result.

<table>
<tr>
<td> 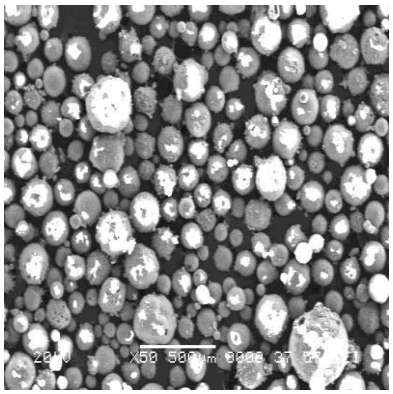
SEM image of Cenosphere</td>
<td> 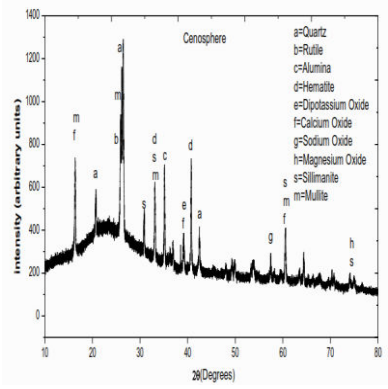

XRD Spectra of Cenosphere</td>
<td> 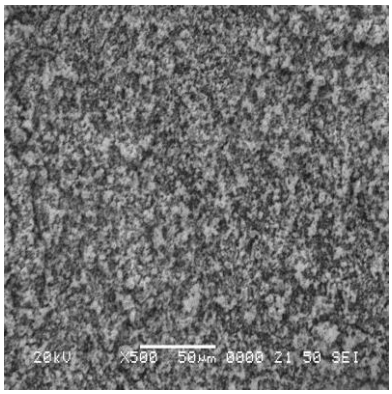
SEM image of TiN powder</td>
</tr>
<tr>
<td> 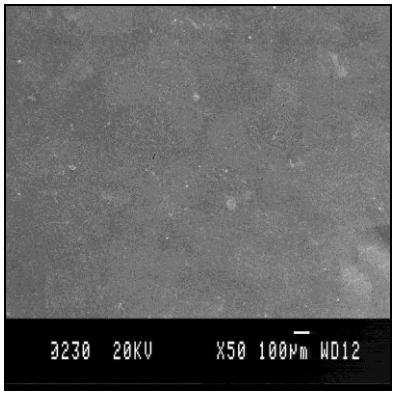
SEM image of Al6061 alloy</td>
<td> 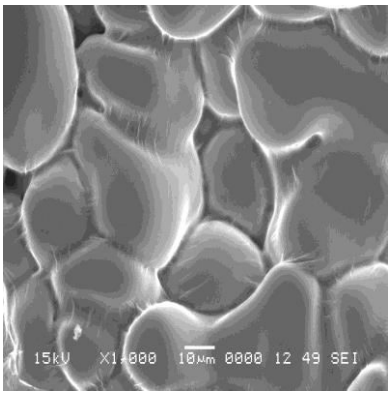
SEM İmage Showing Good Bond</td>
<td> 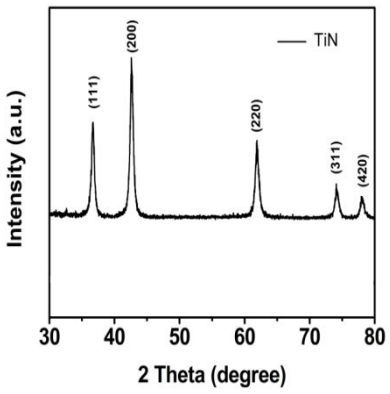

XRD Spectra of TiN</td>
</tr>
<tr>
<td> 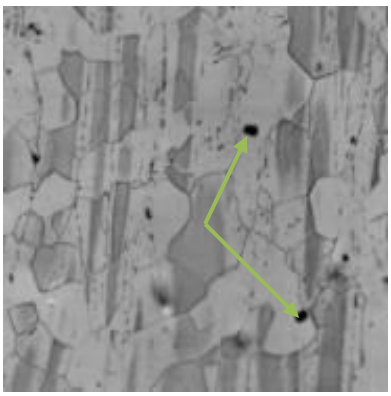
Micrograph of TiN in the matrix</td>
<td> 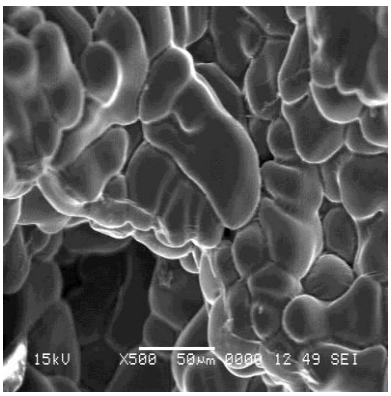
SEM image of Al6061+TiN</td>
<td> 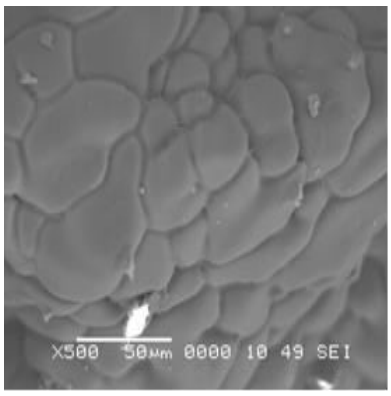
Al6061+15%Cenosphere+1%TiN</td>
</tr>
</table>

3.1 Ultimate Tensile Strength (UTS)

Tensile strength was determined using a 40 kN UTM. Plotting of maximum load versus elongation was done and tensile strength was calculated. The table below shows the effect of cenosphere content on the tensile strength of the composites

Composition	Maximum Load in (kN)	Elongation in (mm)	Tensile Strength (N/mm^2)
Al6061 + 1% TiN	17.5	2	142.6
Al6061 + 1% TiN +5% Cenosphere	18.5	1	150.75
Al6061 + 1% TiN +10% Cenosphere	20	1.5	162.97
Al6061 + 1% TiN +15% Cenosphere	21	1	171.12

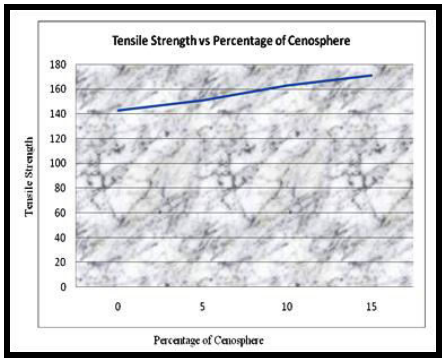

Figure above shows the variation of ultimate tensile strength of Al 6061 matrix alloy and its cast composites. It is observed that all the developed composites have higher ultimate tensile strength when compared with the cast Al 6061 matrix alloy. A maximum improvement of 71.6% and a minimum improvement of 48.51% are observed for Al6061-15wt%Cenosphere-1%TiN and Al6061-5wt%Cenosphere-1%TiN; respectively. The reduced ductility of composites can be due to the stress concentration effects at the matrix and the particle interface.

3.2 Hardness

Figure below shows the variation of micro hardness of Al 6061 matrix alloy and its composites. Micro hardness tests were performed on both Al 6061 alloy and Al6061 -1%TiN and Cenosphere varying from 5wt% to 15wt% in increments of 5%. The micro hardness test was conducted on the polished samples using Vickers Microhardness tester.

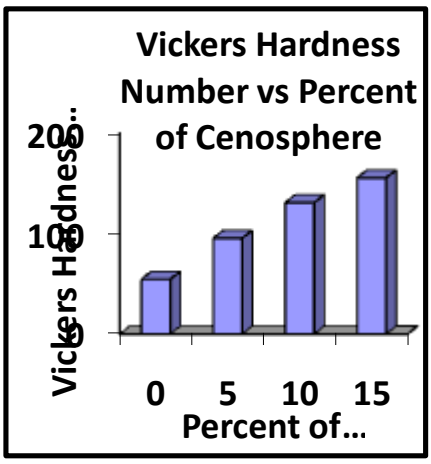

Higher hardness values of Al6061-1%TiN-15wt%Cenosphere composites when compared with base alloy can be attributed to reduced casting defects and improved bond strength/load transfer efficiency between matrix alloy and reinforcement.

IV. CONCLUSION

Good interfacial bonding between the Matrix and Reinforcement can be achieved by using stirring unit in fabrication process and bonding enhances the strength of the composite material. Titanium Nitride can be successfully dispersed in an Aluminium alloy MMC and TiN reinforced Aluminium composite can be obtained. The MMC has got a better hardness when compared with the base metal. This is due to the presence of TiN, cenosphere within the aluminium matrix.MMCs containing up to 15wt% cenosphere (fly ash) particles were easily fabricated. A uniform distribution of cenosphere was observed in the matrix. The hardness increases with an increasing percentage of cenosphere particulates coupled with constant 1%TiN. Similarly the tensile strength increased proportionately with increase in cenosphere content upto 15wt% respectively.

V. ACKNOWLEDGMENT

Our special thanks to Dr.S.Seetharamu, MTD, C.P.R.I, Bengaluru for his valuable suggestions and providing the test material. We express our sincere thanks to Mr.G.N.JaiPrakash, R, D&E, Kennametal, Bengaluru for his references and S.E.M. preparation during the course of this work. We are thankful to Mr.Sudhindra and Mr.Rajkumar Mutgi, R.S.M.L, Bengaluru for providing us their lab for this project to analyze the results. My thanks and regards also go to research community in developing the article and people who have willingly helped me out with their abilities.

REFERENCES

[1]. Rittner M., 2000. Metal matrix composites in the 21st century: markets and opportunities. BCC Inc. Norwalk, CT.

[2] Das S, "Development of Aluminum Alloy Composite for Engineering Applications", Indian Institute of Materials, Volume 27, No. 4, pp. 325-334, August, 2004.

[3] Surappa M.K, Rohatgi P.K, "Preparation and Properties of Cast Aluminum-Ceramics Particle Composites", Journal of Materials Science, Volume 16, pp. 983-993, 1981.

[4] Darell R, Herling G, Glenn J and Wrrent H.Jr, "Low Cost Metal Matrix composites" Journal of Advanced Materials and Process, pp. 37-40, July, 2001.

[5] Hashim T, Loony L, and Hashmi M.S.J, "Particle Distribution in Cast Metal Matrix Composite", Journal of Materials Processing Technology, Part-1, Volume 123, pp. 251-257, 2003.

[6] J.W. Kaczmar, K. Pietrzak, (2000) "The production and application of metal matrix composite materials" Institute of Mechanical Engineering and Automation, Technical University of Wrocoaw, Poland Institute of Electronic Materials Technology, Journal of Materials Processing Technology (106) 58-67.

RFID TECHNOLOGY: CASE STUDY OF ITS MULTI-APPLICATIONS IN WIRELESS COMMUNICATION

Prof.[Dr.] K. K. Saini[1] , Sanjay[2], Shashank[3], Anita[4], Seema[5]

[1,2,3,4,5]*Dronacharya Engineering College Gurgaon, Gurgaon,(India)*

ABSTRACT

RFID technology was developed in early 19th century but in the past few years, this technology went from being unimportant to orthodox applications. RFID technology provides more detailed visibility and tracking of assets and inventory and offers deliberate advantages. Initially, some virtual database with RFID tags, antenna and readers were created and verified. Then research and experiments were conducted to find trends in scientific and virtual environments. RFID provides detection from a relative far distance unlike bar code system. It does not even require product or asset to be in line of sight. In this paper, we discuss about basic working of RFID system, its evolution, some applications and limitations of this technology which need to be overcome to make it more efficient to use.

Keywords: Scanning Antenna, Transponder & Radio Frequency Identification

I. INTRODUCTION

Radio Frequency IDentification (RFID) is a technology that employs a microchip with an antenna that broadcasts its unique identifier and location to receiver. In this technology, radio frequency electromagnetic fields are used to transfer data to identify and track automatically the tags attached to various objects. These tags usually contain electronic information. RFID system can be used just about anywhere, from clothing tags to missiles to pet tags of food- anywhere that a unique identification system is needed. The tag can carry information as simple as a pet owner's name and address to as complex as instructions on how to assemble a car. Some auto manufacturers use RFID system to move cars through assembly line. At each successive stage of production, the RFID tag tells the computer what the next step of automated assembly is.

Any application of RFID needs to result in obvious business benefits. The last few years have seen several developments that have sped up the adoption of this technology:

- The emergence of major consumer applications that bring RFID from an experimental technology into the mainstream. As it gains understanding and credibility through highly visible consumer applications that prove its effectiveness, its place as a solution in supply chain automation also grows.
- The development of "smart labels"—a lower cost, easily integratable version of RFID tags that is beginning to take off on paths where bar codes cannot travel.

II. HOW RFID WORKS?

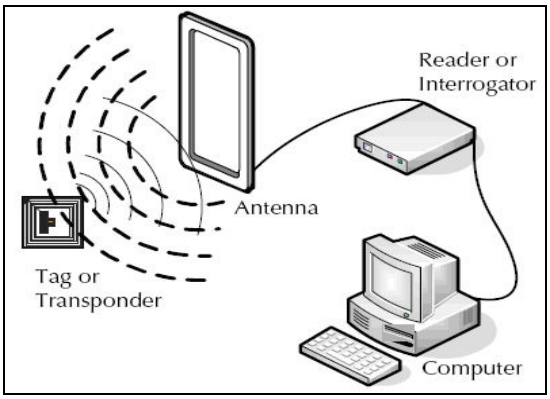

The RFID system has three components, these are:

- Scanning antenna
- A transreceiver with decoder to interpret the data.
- A transponder- a RFID tag – that has been programmed with information.

The RF radiation does two things:

- It provides a means of communicating with the transponder, and
- It provides the RFID tag with the energy to communicate (in case of passive RFID tags).

The scanning antennas can either be affixed to one place or they can be used as handheld antennas. For example, we can build them into door frames and accept the data from the persons or objects passing through the door. When RFID is brought in the field of antenna, it detects an activation signal from antenna and then it transmits the information on its microchip that is received by scanning antenna.

The signalling between reader and antenna depends on the frequency band used by the tag. The tags which operate on LF and HF are small percentage of wavelengths away from reader antennas. In this region, the tag gets cupled electrically with the reader and it modulates the field produced by reader by changing the electrical loading(represented by tag). Then because of switching in relative loads, the tag produces the change which is then detected by reader.

In case of UHF and higher frequencies, the approaches are different as the tags and readers are more than one radio wavelengths away. So, the tag may backscatter a signal. Active tags may contain seperated transmitters and receivers and the tag need not respond on a frequency related to the reader's interrogation signal.

III. TYPES OF RFID TAGS

The RFID tags can be of following types:

- Active Tags: these tags have their own internal power sources. Many active tags operate at fixed intervals. These tags are also called beacons as they broadcast their own signals. These tags have an advantage that the reader can be far away from the tag and still get signals. They have limited life spans, say upto 10 years.
- Passive Tags: these tags have no internal power supply. These tags, however, do not require any batteries and can be much smaller and have a virtually unlimited life span. In these tags, electrical current induced in antenna by the incoming signal proves power for integrated circuit in tag to power up and transmit response.

- Semi-passive Tags: these tags are similar to passive tags, with addition of a small battery. The external battery provides power to integrated circuit. They have longer range but limited lifespan.

The folloiwng table explains more about the difference between these types of tags:

Tags and Features	Passive Tag	Active Tag	Semi Passive Tag
Internal Power Source	No	Yes	Yes
Signal by backscattering the carrier wave from the reader	Yes	No	Yes
Response	Weaker	Stronger	Stronger
Size	Small	Big	Medium
Cost	Less expensive	More expensive	Less
Potential Shell life	Longer	Shorter	Longer
Range	10 centimeters to few meters	Hundreds of meters	Hundreds of meters
Sensors	No	Yes	Yes

IV. RFID V/S BAR CODES

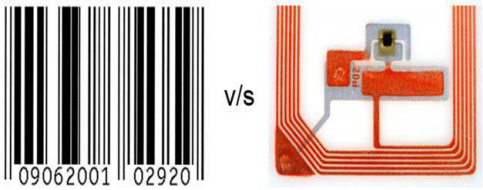

With the different sectors using the two forms of automated data collection i.e. barcode and RFID systems, there is much hype as to whether RFID will take over to barcode system. It is not compulsory that new methods are always essentially better than old ones. These two both carry product information however they both differ a great amount.

To know the difference between barcode and RFID system, first we should discuss what is a bar code.

What is a bar code?

A barcode is visual representation of data that is scanned and interpreted for information. Each bar code contains a certain code which works as a tracking technology for products. Originally this technology used the difference in width and spacing in parallel lines and its considered as one dimensional. Later it evolved into other two dimensional shapes like hexagonal and rectangular shapes. These barcodes can be scanned by barcode readers or by smartphones also.

Now, the difference between the two technologies is explained below:

Barcode	RFID
Require line of sight to be read	Can be read without line of sight
Can only be read individually	Multiple tags can be read simultaneously
Cannot be read if damaged or dirty	Can cope with harsh or dirty environments
Can only identify the type of item	Can identify a specific item
Cannot be updated	New information can be over-written
Require manual tracking and therefore are susceptible to human error	Can be automatically tracked removing human error

V. HISTORY OF RFID

[10] This technology was first used in world war II by american forces to identify enemy aircrafts and tanks. The systems deployed at that time are still being used in defence sector.

With time, the systems were further developed leading to technology expansion. For e.g. in 1970s RFID technology was being used to identify railroad cars or automobile parts in paint shops. Afterwards, electronic article surveillance appeared that was first large scale system of its kind in the market. The main function of this system was to guard against thefts in goods and clothings. The technology became known to a wide public a few years ago when large supermarket concerns decided to document the delivery chain of their goods by means of RFID. Since then there have been many reports on RFID in the media, and its use has also frequently been the subject of controversy.

VI. APPLICATIONS OF RFID

There are various applications of RFID technology emerging nowadays. Some of these are explained as follows:

- ASSET TRACKING: Earlier, static or in motion asset tracking or locating was not an easy task. But now, user can instantly determine general locations of tagged assets anywhere within the facility with the help of active RFID technology. Control point detection zones at strategic locations throughout the facility allow the user to define logical zones and monitor high traffic areas. Tagged assets moving through these control points provide instant location data. Asset tracking applications will see an almost vertical growth curve in the coming years and the growth rate in this area will be much higher than the growth rate of general RFID market.
- PEOPLE TRACKING: this is similar to asset tracking system. Hospitals and jails can be the most required places for this type of tracking. Hospitals employ this technique in tracking some special patients, emergency cases and essential equipments. Mental hospitals can also use this to keep an eye on every patient. This technology can be used best in jails, where every inmate can easily be tracked and located and then no jail inmate will try to escape.
- DOCUMENT TRACKING: with the availability of large amount of data and documents, it becomes difficult to keep manual records and locations of that data and documents. With introduction to RFID technology, both time and money can be saved because this will save: 1) time spent to search the lost documents and 2) the financial and legal impact related with document losses.
- GOVERNMENT LIBRARIES: this technology can also be used in various libraries. RFID technology can read multiple items or assets simultaneously which helps in reducing queues and increase the number of customers using self check. This result in reduction of the staff required at circulation desks.
- MANUFACTURING AND PRODUCTION: this technology gives out an easy way to manage huge manufacturing and production processes. This offers all benefits of small production parts to batch, processing and manufacturing. This helps in reducing time to locate parts and products, reduce and eliminate bottlenecks, and results in better analysis.

VII. LIMITATIONS OF RFID

Even though this technology has been developing over the years, but it has certain barriers or limitations that still need to be neutralised to make effective and easy use of this technology. These problems may be related to investments, security risks and some others. These are as follows:

- COST: although there is great potential in RFID technology, but its relative high cost is a drawback. RFID tag is comparatively costlier than barcode system. Besides the initial cost, there is a cost to be invested in

maintainence of the system also. In future, when prices are reduced then more retailers and manufacturers can implement this technology and then it will overcome the barcode system completely.

- SECURITY AND PRIVACY: this limitation has been a part of debate from the beginning. It will certainly violate the customer privacy as it can easily the person using the product.The tags(RFID tags) when used, may broadcast the EPC(electronic product code). For example, the size of the dress a woman wants to wear will be sent publically to the nearby reader by RFID tag. Many suggestions are being given to overcome this problem, simplest is " kill tag" in which the tag is electronically deactivated after the sale mof the item. Some other solutions are crptographic approach, hash function approach, faradey cage approach, active jamming approach, regulation approach etc.
- INTERFERENCE: since RFID is based on rado frequency technology, it can be easily interfered with some other radio wave transmissions occuring over the same place, or it can be interfered with some metals,liquids etc. the degree of interfernce depends on the frequency of tag and usage environment.
- LACK OF STANDARDISATION: RFID is still in initial stage and there are many hurdles ahead of it. At present, there are many different RFID systems that operate upon different frequencies and need different softwares and readers. So, the need is to be agrees upon that only one or group of frequencies have interoperability between the manufacturers, retailers and distributers.

VIII. CONCLUSION

For now, RFID technology can't overcome barcode technology completely because of its accuracy, cost and other limitations. Some large companies like tesco, prada, benetton, wal-mart etc are making use of this technology and they are exploring the impact also. Other industrialists can also use this technology. The base of success of this technology lies in understanding the technology and its features deeply to overcome its limitations and potential problems.

REFERENCES

[1]. www.ti.com/rfid/docs/manuals/whtPapers/manuf_dist.pdf
[2]. www.ftc.gov/bcp/workshops/rfid/juels.pdf
[3]. http://www.aalhysterforklifts.com.au/index.php/about/blog-post/rfid_vs_barcodes_advantages_and_disadvantages_comparison
[4]. http://www.rfidsurvival.com./
[5]. http://www.iaeng.org/publication/WCECS2009/WCECS2009_pp1253-1259.pdf
[6]. http://www.scirp.org/journal/PaperInformation.aspx?paperID=2578
[7]. http://www.cse.wustl.edu/~jain/cse574-06/ftp/rfid.pdf
[8]. http://www.roywant.com/cv/papers/2006/2006-01%20(IEEE%20Pervasive)%20GE%20RFID%20(print).pdf
[9]. http://www.stitcs.com/en/RFID/RFIDResearchTrends.pdf
[10]. http://www.brooks-rfid.com/rfid-history.html
[11]. http://www.indiantextilejournal.com/articles/FAdetails.asp?id=478

International Conference on Recent Innovations in Science, Engineering and Management
YMCA, New Delhi, 30th May, 2015 ISBN: 978-81-931039-4-4

MATHEMATICS: PROBLEM OR OPPORTUNITY? IN TECHNOLOGICAL PROGRESS AND ENGINEERING EDUCATION

Kirti Rani

Ex. Lecturer, Department of Mathematics, Govt. P.G college Ambala Cant., (India)

ABSTRACT

Technology has become a major force that transforms and adds new dimensions to our lives. Technological progress can both create problems as well as solve them. There is a close relationship between engineering, mathematics and technological progress in the context of education. A major question is that which type of education we provide to Engineering students so that they can takes mathematics as an opportunity not as a problem. We should develop a practical understanding of how we are influenced by mathematics and technology and how our choices as workers, consumers and citizens influence technological progress in future. Mathematics is an essential tool for engineering, so it should taught with more application based examples. We found technology should be taught to students in an integrated manner with mathematics .Engineers are thoroughly educated in mathematics and sciences ,and applies the knowledge to design and develop usable techniques, structures and processes.

I. INTRODUCTION

The pace of technological progress has significant implications on local and global economies, societies and institutions. The convergence of technology with industry and the sciences will raise tough questions on the future of our society. And so in future we will need professional engineers with great interdisciplinary understanding, and with more skills. Engineers will require frequent updating in area of their specialization in this rapid pace of technological changes. There will be a great diversity, but all will need a deep understanding of sciences that underpin the art of engineering, and all will therefore need the mathematical skills needed to apply these sciences. A deep understanding of mathematics is an essential weapon for modern engineers. Mathematics is the mother of all sciences and governs the World of economics, Finance, social sciences etc. and what not. An engineer can be a good and successful Engineer, only if he is good in mathematics. We are living in a world of rapid change — reflected in technology shifts, global volatility and emerging opportunities. Advances in the use of information technology have transformed the analytic techniques of engineering. These advances will surely continue, creating opportunities for all engineers, in two ways of knowledge can be acquired, and then applied. The role of mathematics in engineering education and technological development is one of these opportunities. The major part of motivation for research is the fact that in India, the mathematical education of engineers is a topic of increasing debates. Nevertheless, explicitness doesn't necessarily imply that an engineer's understanding of mathematics cannot also be situated in the objects and tools of engineering practice and describing this has been a major concern of our research.

II. RESEARCH STRATEGY

We undertook interviews and observations of students and professors in many Institutions of technology in India. An extensive literature search was also undertaken, beginning with the proceedings of engineering and mathematical education conferences. A questionnaire was also designed to explore the themes identified by the experts.

III. HISTORY

Over the last forty years science, technology and mathematics education have emerged as lively new research areas. The research activity in these areas has been reflected in the launching of literally hundreds of new journals, in science education, mathematics education and, more recently, in design and technology education. Much of this research is carried out at the primary, middle and secondary levels of schooling. In the past, engineers had to learn a lot of mathematics for practical purposes. At the same time, they could be expected to absorb some more meta-level knowledge about mathematics as a 'logical way of thinking', and the importance of that way of thinking as part of a practicing, alongside practical experience, physical and intuitions, codified knowledge of profession.

IV. FINDINGS

New trends to 'knowledge' are developing in engineering education. Technical knowledge has expanded, and is expanded, at a great rate. In the nineteenth century it would have been feasible for all of the needed technology for professional engineer to have been covered in a conventional engineering course. The importance of a serious mathematical education for engineers was highlighted in many studies. It is impossible for any institute to cover all of the needed technology. Some institutions have developed software which allows students, or in some cases forces to practice mathematics with feedback on errors [7]. The mathematical techniques should be applied to a range of problems encountered in process of technological reforms and progress by engineers. In this era of advanced technology, education system should increase the quality of educational offering in mathematics, science and technology at all grade levels. Mathematics, science and technology are of course intimately connected: at theoretical as well as practical and application levels, engineering, technology progress and mathematics (METP) are linked via intricate networks of concepts.

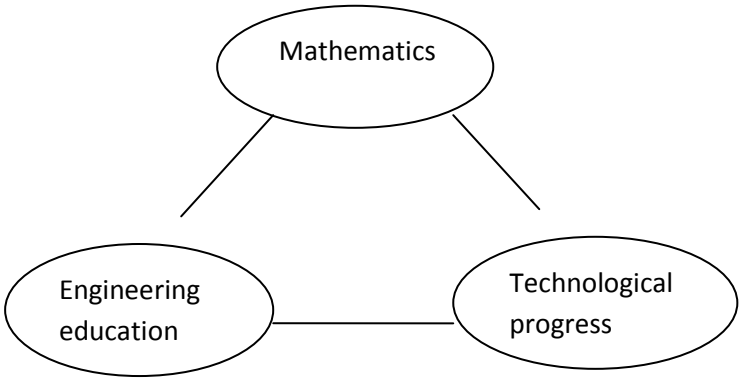

Now we find, in investigating the educational issues in METP, that there are a multitude of further uniting themes that originate in the cognitive, pedagogical, aspects of Science, Technology and Mathematics Education (METP).

V. MATHEMATICS: PROBLEM OR OPPORTUNITY?

In our survey we have found that most of the students take mathematics as a problem of their curriculum, but the fact is that they don't understand the main role of mathematics in their education, the motive of students is only to get passing marks in mathematics. They don't understand that mathematics is not a problem, but it helps to solve the problems, it is an opportunity for them. In order to resolve the apparent contradictions of mathematics as problem or opportunity, it is necessary to consider the different uses of mathematics in engineering practice. Mathematics is and will remain crucial, and this paper addresses some questions facing engineering mathematics education:

- What type of mathematics knowledge do engineers need?
- What and how mathematics should be taught?

VI. PROBLEMS RELATED TO MATHEMATICS EDUCATION FACED BY INSTITUTES OF TECHNOLOGY

Increased number of institutions of technology has lowered the entry standards for students; it leads to the increased diversity of students of mathematical backgrounds. Also, there is a lack of mathematics staff and mathematics labs, therefore students can't understand the practical use of mathematics and unable to use mathematical concepts in further technological progress. We are much attracted by the concept of mathematics being pulled rather than pushed into engineering context. Students are perceived to lack fluency in algebraic manipulation, and to lack a proper appreciation of what mathematics is about in terms of the roles of precision and proof.

VII. SUGGESTIONS TO OVERCOME THE ABOVE MENTIONED PROBLEMS

To overcome the difficulties faced by the students, the educationists and institutions should begin new methods like:

- Project base learning.
- Visual sources.
- Mathematical software programs.
- Online instructional materials.
- Flexible, formative and summative assessment. Continuous assessment forces the student to have the control of his own learning and choosing the best method to show his success as much as possible [1].
- Use of advanced computer based methods for mathematics teaching.
- There should be proper mathematics laboratories.
- Good and eligible mathematics staff.
- Address student variability.

- Use a problem based learning strategy [5].
- Cooperative learning in engineering mathematics would be an efficacious method for engineering students in mathematics learning [4].

A research agenda needs to be established on what are the norms for technology mathematical and engineering literacy. It is necessary to consider the different use of mathematics in engineering practice: the direct usefulness of mathematical techniques and ideas to practice and their indirect usefulness- the ways in which mathematics contributes to the development of engineering expertise and judgment.

VIII. BRANCHES OF MATHEMATICS FOR ENGINEERS

To improve mathematics education in engineering studies, some new branches of mathematics are important which helps the student to understand how to use mathematics in solving problems. The mathematics and sciences, as well as the technical courses, in technology programs are taught with more application based examples. Engineering courses may also require additional, higher-level mathematics, including multiple semesters of calculus and calculus-based theoretical science courses to prepare students for continued studies and perform research at the graduate level. Mathematics demands careful thought sustained attention and practice to an extent that students become influent and at ease in their handling of formulae, equation and geometry [9]. Engineering technology courses generally have labs associated with the courses that require hands-on applications of the studied topics. Mathematics is a toolbox which is filled with useful tools such as partial derivatives, topological spaces, set theory, group theory, linear transformations, initial boundary value problems, mobious transformations, tolerance spaces and so on. But some major branches and topics of mathematics we discussed here which has an important role in engineering curriculum.

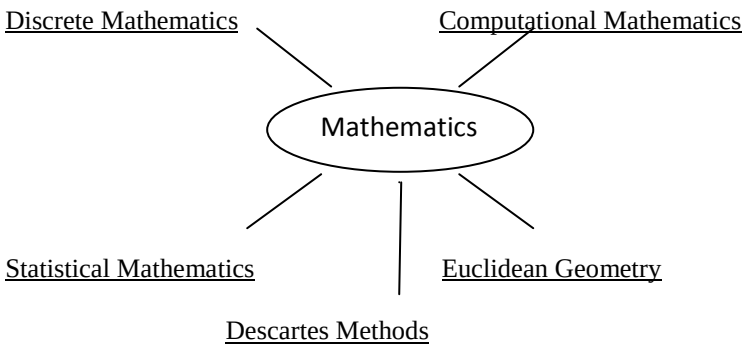

8.1 Discrete Mathematics

Development of continuous mathematics has given an extremely powerful tool called discrete mathematics for handling such problems. Computers have become reality because of technological growth and computers are becoming more and more useful in dealing with problems of discrete mathematics. Today, discrete mathematics is the fastest growing field in modern mathematics. Discrete mathematics should be viewed as part of mathematics that is concerned with determining the nature of discrete structures of various phenomena occurring or prevalent around us in real life. It is this character of discrete mathematics that has made its study not only essential, but also theoretically intriguing and interesting. Its varied applications are simply mind-boggling as they cut across almost all disciplines of knowledge. Discrete mathematics is the fastest growing

field in modern mathematics. It studies the nature of discrete structures of various phenomena occurring in real life.

8.2 Computational Mathematics

Yet the role that mathematics plays in professional practice has changed in last twenty years. Today, 'computational mathematics' is rising as a tremendous opportunity, pushing forward the boundaries of engineering. Within this, mathematics as explicit work by individual engineers has evolved into mathematics as a distributed activity across designing teams and computers that support them. The success of modern numerical computer methods and software has lead to the need of computational mathematics, which occasionally uses high performance computing for the simulation of phenomena and solution of the problems in the science and engineering.

8.3 Statistical Mathematics

The Engineering Mathematics and Statistics major offers students an opportunity to study pure and applied mathematics as essential components of modern engineering. By combining courses for pure mathematics, applied mathematics, statistics, the physical sciences, and engineering, a student may individualize a program of study, of theory, or applications of both. It provides a broad foundation for graduate studies in theoretical branches of engineering, as well as in mathematics, and can prepare students for a carrier in specific sectors of industry or business.

8.4 Descartes Methods

Descartes is one of the most important founders of modern mathematics. Its most important contribution is the creation of the most important part of mathematics used by the engineers: Analytic geometry. Analytic geometry was done by the invention of the coordinate axis for locating a point in space. It de facto merges two previously independent field of mathematics: algebraic and Euclidean geometry. Now algebraic equations correspond to surface and curve in space. It allows to create a dimension of time and de facto create space time and within this framework calculus and differential equations. Be invented and the project of the geometrisation of the world began and the rest is history.

8.5 Euclidean Geometry

Mechanical engineering just needs Euclidean geometry for what they do while for GPS positioning the slight curvature of space-time cannot be neglected and Riemannian geometry is necessary. For crafting nuclear weapon, and understanding chemical reaction and designing microchips regular quantum mechanics is good enough. But cosmologist and astro-physicist would need a quantum gravity theory in order to go back in time at the origin of the cosmos and understanding what is going on in black holes or for expanding physics into a more harmonious whole. A small number of physicists are working at the fundamental level. To conceive Newton's physics, we need analytic geometry and calculus. Both general relativity and quantum mechanics emerged around 1927 about fifty years after Riemannian geometry and Hilbert space the two geometrical foundations have emerged. David Deutsch crafted a new geometrical for mathematics: constructor theory and lee semolina also worked to establish new foundations. These theories are very helpful for engineering students for solving problems.

IX. Conclusion

It is time to reconsider 'pedagogical' approaches that can best 'deliver' the mathematical needs of the students. Mathematics could benefit more 'pulled' into the context of design-oriented engineering teaching rather than 'pushed' into the students in the absence of a context. This entails a shift in approach from teaching mathematical techniques towards teaching through modeling and problem solving. Carefully-designed IT use can make it possible to use mathematical idea before understanding the techniques. In the pre-computational era, a strong objection to pull-based mathematics was that to use a mathematical idea properly required a detailed understanding of techniques of its application. But times, and technologies, change. There is a need for national leadership to stimulate and to promote the spread of, the innovative work in curriculum design and delivery currently being carried out by enthusiastic individuals and individual departments. It is the need of the time that nation's education system should have capacity to continue to develop and broaden the pool of students who are well prepared and highly motivated for advanced careers in mathematics, engineering and technology.

REFERENCES

[1] Wood, L. N. & Smith, G. H. (1999). Flexible Assessment. Proceeding of Delta The Challenge of Diversity-A Symposium on Undergraduate Mathematics. Queensland.

[2] Adams, P. A., Kaczmarczyk, S., Picton & DemiAn, P (2007). Improving problem solving and encouraging creativity in Engineering Undergraduates. International conference on engineering Education, Portugal.

[3] Henderson, S. & Broadbridge, P. (2009). Engineering Mathematics Education in Australia. Msor connections 9(1): 12-17.

[4] Johnson, D.W., Johnson, R. T. & Stanne, M. B. (2000). Cooperative Learning Methods: A Meta Analysis. Available: http://www.tablelearning.com/uploads/File/EXHIBIT-B.pdf.

[5] Lopez, A. (2007). Mathematics Education for 21st Century Engineering students: Literature Review. Australian Mathematics Sciences Institutes. Available at: http.//www.amsi.org.au./carrick.php.

[6] Kent, P. and Noss, R. (2000). The visibility models: using technology as a bridge between mathematics and engineering. International Journal of mathematical Education in Science and Technology, 31(1), 61-69.

[7] Judd, K. (1996). Teaching Intermediate Calculus by Computer. Accessed at: http//calmaeth.maths.uwa.edu.au/doc/reports/report1996.html

[8] Bissell C and Dillon C, 2001, "Telling tales: Models, Stories and meanings", For the Learning of Mathematics, 20, 3, 3-11

[9] Payle, I (2002), 'Prevention is better than cure – Changes needed to A level Mathematics'. Presented at the conference Tackling Mathematics and student Issues in Engineering, University of Glamorgan, Feb. 2002.

[10] Kent P and Noss R, 2001, "Finding a role for Technology in Service Mathematics for Engineers and Scientists". In D Holton et. al (eds.), "The Leaching of Mathematics at University Level: An ICMI study", kluwer academic publishers.

CLASSIFICATION OF PADDY LEAF DISEASES USING SHAPE AND COLOR FEATURES

Suman T[1], Dhruvakumar T[2]

[1]*M.Tech student, Signal Processing, Siddaganga Institute of Technology, Tumakuru, Karnataka, (India)*

[2]*Asst. Professor, Dept. of Electronics and Communication, Siddaganga Institute of Technology, Tumakuru, Karnataka, (India)*

ABSTRACT

Farmers experience great difficulties in early disease detection and it is a major challenge in agriculture field. Automation of essential processes in agriculture is becoming widespread, especially when fast action is required. In this work suitable preprocessing techniques are applied and using histogram plot, normal and diseased leavesare classified. For the diseased leaf, shape and color features are extracted and the combined features of color and shape are used for the classification of bacterial leaf blight, brown spot, narrow brown spot and rice blast diseases using SVM classifier.

Keywords*: *SVM classifier, shape features, color features, bacterial leaf blight, brown spot, narrow brown spot and rice blast.

I. INRODUCTION

Agriculture has always been the mainstay in economy of most of the developing countries, especially the ones located in South-Asia. The purpose of agriculture is not only to feed ever growing population but it's a solution to solve the problem of global warming and it is an important source of energy. India is an agricultural country wherein most of the population depends on agriculture. Research in agriculture is aimed towards increase of productivity and quality of the food at reduced expenditure, with increased profit. Therefore, detection and classification of diseases is an important and urgent task.

The amount of crops that are damaged every year, due to adverse climatic conditions or invasion of pathogens, can never be neglected. Hence, it is important for the farmers to detect the growth of disease in plant at an early stage, and take necessary steps in order to prevent it from spreading to others parts of the field.

Rice is a globalized staple food. It is one of the three leading food crops in the world which makes it a more significant food item worldwide [1]. Rice (Oryzae Sativa) is considered as the main crop in the east India and believed to be the second central crop after wheat, in the world. In a third world country like India where the major staple food is "Rice" where life of many people, economy of the country is related to the production of paddy. Any negative effect on the yield in unwanted. The paddy production can be hampered as effect of some mechanical damage, nutritional deficiency, genetically disorder, climatic conditions etc [5]. But the major problem is disease causing by macrobes [2] and microbes. The disease is easily recognized by their symptoms-changes of the plants.

The efforts to increase the quantity and quality of rice production to satisfy the increasing needs of rice in India experienced several obstacles, one of which is the attack of the diseases on paddy fields. To control these diseases and to minimize the impacts of the attacks, the diseases must be identified quickly. Computer vision is a potential solution to tackles this problem. One way to identify the diseases in plants is by observing the physical changes (diseases spots or lesions) caused by chemical changes in the sick plants. The images of these spots can be processed and used to recognize the diseases quickly, easily, and inexpensively.

The most two common diseases in the North East India are named as Leaf Blast and Brown Spot. The samples of the infected rice leaves have been collected from different parts using Nikon COOLPIX P4 digital camera. Acquired images transformed to Hue Intensity Saturation (HIS) model for segmentation [3]. Entropy based bi-level thresholding method has been invoked for segmenting the images to facilitate identifying the infected parts of the leaves [4].

The RGB color images of paddy leaf are captured using a Canon Power Shot G2 digital camera [5]. The image segmentation based on gray-level threshold segmentation is adapted and the binary image is gained. The main objective of segmentation process is to obtain the binary image with less noise or noise free [6]. The RGB image is converted into a binary image using threshold method. Local entropy threshold method of Eliza and Chang [7] and Otsu method is used for the segmentation [8]. An occurrence matrix is generating from the input image in accordance with probability distribution needed for entropy measures. Five characteristics of lesion i.e., percentage, lesion type, boundary color, spot color, and broken paddy leaf color were tested for the classification task Color is an important sign in recognizing different classes [9].

Four characteristics of lesion type, boundary color, spot color, and broken paddy leaf color were tested for used to establish the classification system. The ratio of height and width of the lesion spot provided a unique shape characteristic for determining the type of the lesion [6]. Generally, the color difference is evaluated using the distance between two color points in a color space. The most common distance is Euclidean distance [6]. Our proposed technique is based on the CIELab color space, which is a uniform chromaticity color space to get boundary color, spot color and broken leaf color. It is known that Euclidean distance of two colors is proportional to the difference that human visual system perceived in the CIELab color space [7][10].

A probabilistic neural network (PNN) is nonparametric classifiers [11]. PNN work faster than the back propagation neural network, even up to 200,000 times faster as it only needs one iteration of training process. Training and testing data were splitted using 5-fold cross validation. The results were presented using confusion matrix for further analysis.

In this present work four different types of paddy diseases are considered namely, brown spot, narrow brown spot, bacterial leaf blight and leaf blast. Here, bacterial leaf blight and narrow brown spot has the similar shape and rice blast, brown are almost similar in color, hence both the color and shape features are used for the classification purpose.

II. DISEASES OF PADDY LEAVES

Rice plant is distress from many diseases [1], [2] the main diseases are caused by bacteria and fungus. The RGB normal rice leaf is shown in Fig 1(a). The diseases which are considered in this work are listed below

2.1 Brown spot

It is caused by the virus named as Cochliobolusmiyabeanus &Helminthosporium. Brown spot diseased leaf is shown in Fig 1(b). The main symptoms are

- Initially appears as brownish spots on leaves.
- Later, it becomes Oval shaped foliar spots with yellow halo.
- The spots are brown, with greyish centers when fully developed.
- Appear in leaf blade & sheath

2.2 Narrow brown spot

It is caused by the virus named as Cochliobolusmiyabeanus&Helminthosporium. Narrow Brown spot diseased leaf is shown in Fig 1(c). The symptoms are similar to the brown spot but these are long and narrower when compared to brown spot diseased part.

2.3 Bacterial leaf blight

It is caused by the bacteria named as Xanthomonasoryzae_andpv. Oryzae. : Bacterial leaf blight diseased leaf is shown in Fig 1(d). The main symptoms are

- Water soaked lesions move from tip downwards on the edges of leaves.
- Gradually symptoms turn into yellow and straw colored stripes with wavy margins.
- In early morning in humid areas yellowish, opaque, turbid drops of bacterial ooze may be seen.

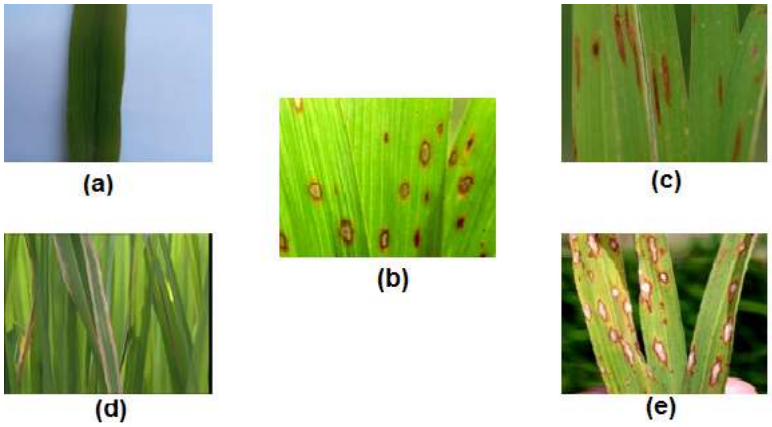

Figure 1: RGB image of normal leaf (a), (b)-(e) diseased leaves of brown spot, narrow brown spot, bacterial leaf blight,, rice blast respectively.

2.4. Rice Blast

It is caused by the fungus named as Pyriculariagrisea. Rice blast diseased leaf is shown in Fig 1(e). The main symptoms are

- Start as small water soaked bluish green specks.
- Leaf spots are typically elliptical (football shaped), with gray-white centers and brown to red-brown margins. Fully developed leaf lesions are approximately 0.4 to 0.7 inch long and 0.1 to 0.2 inch wide.

III. PROCESS DESCRIPTION

Different types of diseased and normal paddy leaves are captured using digital camera. After that an image is cropped manually in such a way that it contains both healthy and diseased part in it. It is the only manual work involved in this process and this image is given as input to the further process. The block diagram of proposed

work is shown in Fig 2.In image pre-processing green plane is extracted to enhance the diseased part. The major objective of preprocessing stage can be to reduce the amount of noise present in the document and to reduce the amount of data to be retained. Median filter is used in order to remove the noise present in the acquired image. Diseased part of the leaf image need to be extracted by using suitable segmentation technique. The features of the segmented image are extracted in order to recognize the different diseases. Then the data extracted in the features are stored in the database.

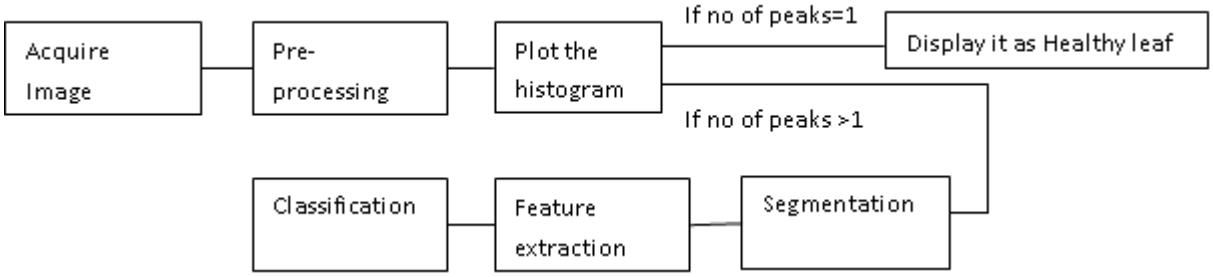

Figure2: Block diagram of proposed leaf disease detection and classification

3.1 Preprocessing

Image preprocessing is the name for operations on images where it can be used to improve the image data that removes the background noise and also suppress the undesired distortion. Through various image preprocessing steps, image features for processing and analysis are enhanced. The preprocessing steps involved in this work are represented in Fig.3.

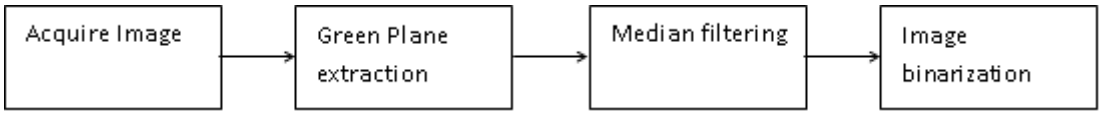

Figure 3: Block diagram of preprocessing steps involved in the proposed work

3.1.1. Acquisition of images

Acquire the images of normal and diseased leaf using digital camera with a white background. Images are taken with a white background in order to avoid the reflections while capturing the images.

3.1.2. Green plane extraction

Acquired RGB imageis used for further preprocessing involved in the proposed methodology. It can be easily observed that greenness of the leaf is more affected when the infection is occurred in leaf. Extract the green color component in order to enhance the affected portion of the leaf. Instead of considering only the green values, intensity of the original gray scale image is subtracted by the green value so that the spot detection is invariant of the brightness and age of the leaves.

3.1.3. Median filtering

Median filter is nonlinear in nature and it is a smoothening filter. Here, it is used to preserve the edge information as it had a less blurring effect when compared to the other smoothening filters after applying on to the image. Median filter is applied to remove unnecessary spots. As a result, a noise free grayscale image is produced. It replaces the value of the center pixel, by the median of the gray levels in the image area enclosed by the filter. In order to perform median filtering, first window is moved and all the pixels enclosed by the window are sorted. After then median is computed and this value is assigned to center pixel. If the number of elements in 5X5 window is odd, middle value is assigned as median value, else average value is assigned as

median value, and else average of two middle values is assigned as median value. Median filtering operation is shown in Fig.4.

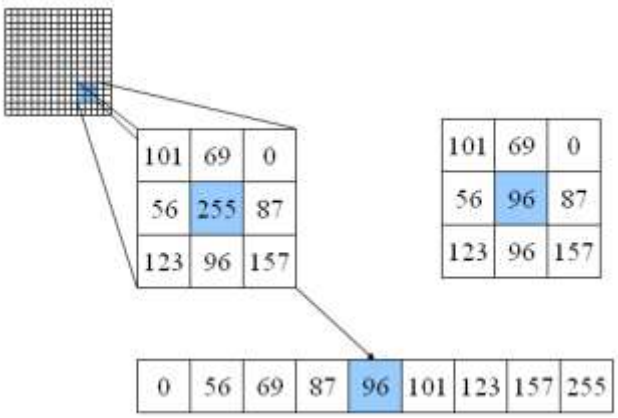

Figure 4: Kernel showing the median filtering operation

3.1.4. Binarization

Thresholding is used to convert a gray scale image into the binary image. Thresholding technique replaces all pixels of an input image with black pixels if the intensity $I_{x,y}$ less than some fixed threshold T or a white pixel if the intensity is greater than the fixed threshold T.So that the resultant image is binarized by applying the thresholding.

3.2. Classification of healthy and diseased leaf

For an uninfected leaf the distribution of color is nearly uniform while for the diseased leaf the distribution of the color is not uniform because the pixel values of the diseased leaves varies widely and differs from the normal intensity value of pixels. In order to distinguish between the uninfected and diseased leaves a histogram approach has been used. Histogram represents the probability of occurrences of different gray levels in the image. The high probability of a particular gray level corresponds to a peak in the histogram.

Binary image is multiplied with the original gray scale image and the histogram is plot to the resultant image. Count the number of pixels lie in the intensity value greater than zero. If the sum is obtained then the result is unhealthy leaf. If the sum is zero then it is healthy leaf.

In the case of healthy leaf intensity value is lie in only one value so the peak is one and the result will be displayed as healthy leaf. In the case of an diseased leaf pixel intensity spread in all intensities so the peak is greater than one and hence it is displayed as unhealthy leaf.

3.3. Segmentation

Image segmentation is the process of partitioning a digital image into multiple segments. The goal of segmentation is to simplify and change the representation of an image into something i.e. more meaningful and easier to analyze. The result of image segmentation is a set of a segment i.e. collectively cover the entire the image or set of contour extracted from the image. The main idea of the image segmentation is to group pixels in homogeneous regions and the usual approach to do this is by common feature. Image segmentation is the process of dividing the given image into regions homogenous with respect to certain features for image segmentation. 8-connected component analysis is used for the segmentation of the diseased leaf.

IV. FEATURE EXTRACTION

The main aim of feature extraction is to extract the information that can be used to determine the meaning of the given sample. Shape, color and texture features are the main features that are included in image processing. Here, shape of the infected region and color changes in the lesion area are considered as the features for the classification different kinds of diseases. The color features are influenced by outside light and different diseases of plant leaves had same shape features, hence both color and shape features are considered as the characteristic values of classification of different types of diseases.

4.1. Shape features

Principal Component Analysis is used for shape feature extraction. PCA transforms correlated variables into uncorrelated variables retaining maximum amount of variations. This helps to operate on data and make predictions. Each image is converted into vector and stored as columns of matrix $P \times N$. Mathematically principal components are obtained by subtracting mean from each column. The resultant matrix is given by B.

$$B = [\hat{X_1}, \hat{X_2} \ldots\ldots, \hat{X_N}] \quad (1)$$

Then the covariance matrix S is obtained by

$$S = \frac{1}{N-1} B^T B \quad (2)$$

Thus the dimension of the feature vector reduces to $P \times P$. The eigen values and eigen vectors are calculated using $P^T SP = D$. Where D is the diagonal matrix with eigen values. And P is is a matrix of eigen vectors. Eigen vectors are arranged according to the descending values of the eigen values. The weight matrix W is determined as $W = PB^T$and this weight matrix is used as features for classification.

4.2. Color features

In image processing color features plays very important role and an important sign in recognizing different classes. These color features are very helpful when investigating the lesion for early diagnosis. Here, "Grid based color moments" are used as a feature vector. Compute the color features for a given image using following steps

- RGB image converted into HSV color spaces
- An image is uniformly subdivided into 3X3 blocks
- Compute mean color (H/S/V) for each of the nine blocks

$$x' = \frac{1}{N} \sum_{i=1}^{N} x_i \quad (3)$$

Where N is the total number of pixels within each block,x_i is the pixel intensity in H/S/V channels.

Mean is considered as one of the feature as it measures the average intensity value.

- Compute variance for each block and for each channel

$$\sigma^2 = \frac{1}{N} \sum_{i=1}^{N} (x_i - x')^2 \quad (4)$$

Variance has the capability of measuring the variability as the intensity level get changes at the edges of the images by large value variance can be used to sharpen the edges.

- Compute the skewness for each block of(H/S/V)

$$\sigma^2 = \frac{\frac{1}{N}\sum_{i=1}^{N} (x_i - x')^3}{(\frac{1}{N}\sum_{i=1}^{N} (x_i - x')^2)^{\frac{3}{2}}} (5)$$

Usually skewness is used is used for judging the image surface. It can be positive, negative or zero. Skewness measures the asymmetry of the image.

Each block will have 3+3+3=9 features, and thus the entire image will have 9x9=81 features. Before we use SVM to train the classifier, we first need to combine the shape and color features for claasification.

V. SVM CLASSIFIER

SVM is a powerful discriminative binary classifier which models the decision boundary between two classes as a separating hyper plane. This hyper plane tries to split, one class consists of the target training vector (labeled as +1), and the other class consists of the training vectors from an impostor (background) population (labeled as −1). Using the labeled training vectors, SVM optimizer finds a separating hyper plane that maximizes the margin of separation between these two classes and it is shown in Fig.5.

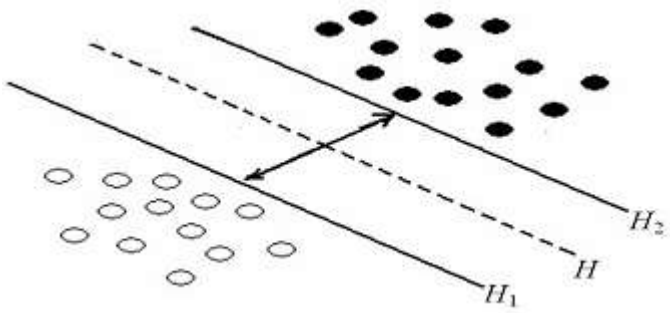

Figure 5: The optimal plane of SVM in linearly separable condition

Formally, the discriminative function of SVM is given by

$$f(x) = \sum_{i=1}^{N} \alpha_i t_i K(x, x_i) + d \qquad (6)$$

Here $t_i \in \{+1, -1\}$ are the ideal output values, $\sum_{i=1}^{N} \alpha_i t_i = 0$ and $\alpha_i > 0$. The support vectors x_i, their corresponding weights α_i and their basis term d, are determined from the training set using an optimization process. The kernel function $K(.,.)$ is designed so that it can be expressed as $K(x, y) = \varphi(x)^T \varphi(y)$, where $\varphi(x)$, is a mapping from the input space to kernel feature space of high dimensionality. The kernel function allows computing inner products of two vectors in the kernel feature space. In a high-dimensional space, the two classes are easier to separate with a hyperplane. Intuitively, linear hyperplane in the high-dimensional kernel feature space corresponds to a nonlinear decision boundary in the original input space. The most widely used kernel functions are: Linear kernel, the Radial Basis Function function kernel (RBF kernel), the sigmoid kernel. Since the real world problem deals with multi class classification. This problem can be solved using two approaches: One-Against-All (OAA) approach and One-Against-One (OAO) approach.

VI. EXPERIMENTAL RESULTS

For the detection and classification of plant leaf diseases, acquire the images of normal and diseased leaf using digital camera with a white background, and this acquired image is passed through different preprocessing steps.

Extraction of green color component of four different diseases i.e., bacterial leaf blight, brown spot, narrow brown spot and rice blast respectively is shown in Fig.6. Median filter is applied to remove unwanted spots and the results when applies to four diseases are shown in Fig.7. Intensity enhanced image in order to enhance the diseased part is shown in Fig.8. Fig. 9 shows the results of binarized image after applying the thresholding. Classification of healthy and disease leaf for healthy, bacterial leaf blight, brown spot, narrow brown spot and rice blast respectively are shown in Fig. 10. Results of segmentation using 8-connected component analysis aregiven in Fig.11.

Figure 6:Green plane extraction of bacterial leaf blight, brown spot, narrow brown spot and rice blast respectively.

Figure 7:Median filtered results of bacterial leaf blight, brown spot, narrow brown spot and rice blast respectively.

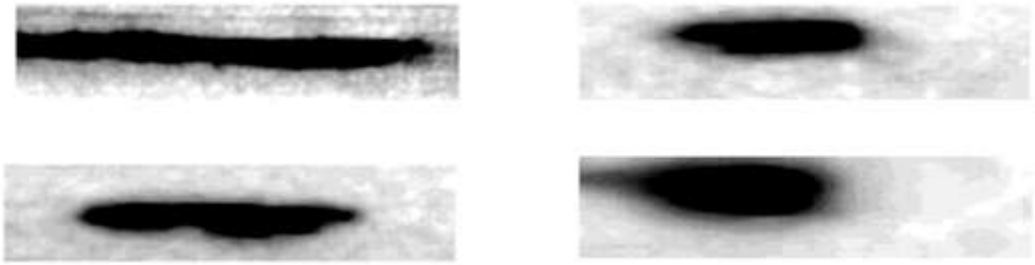

Figure 8:Intensity enhanced results of bacterial leaf blight, brown spot, narrow brown spot and rice blast respectively.

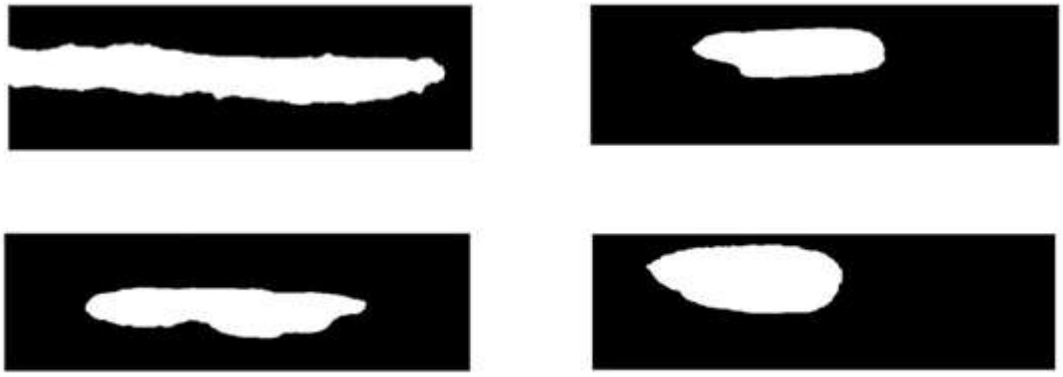

Fig 9: Binarized results of bacterial leaf blight, brown spot, narrow brown spot and rice blast respectively

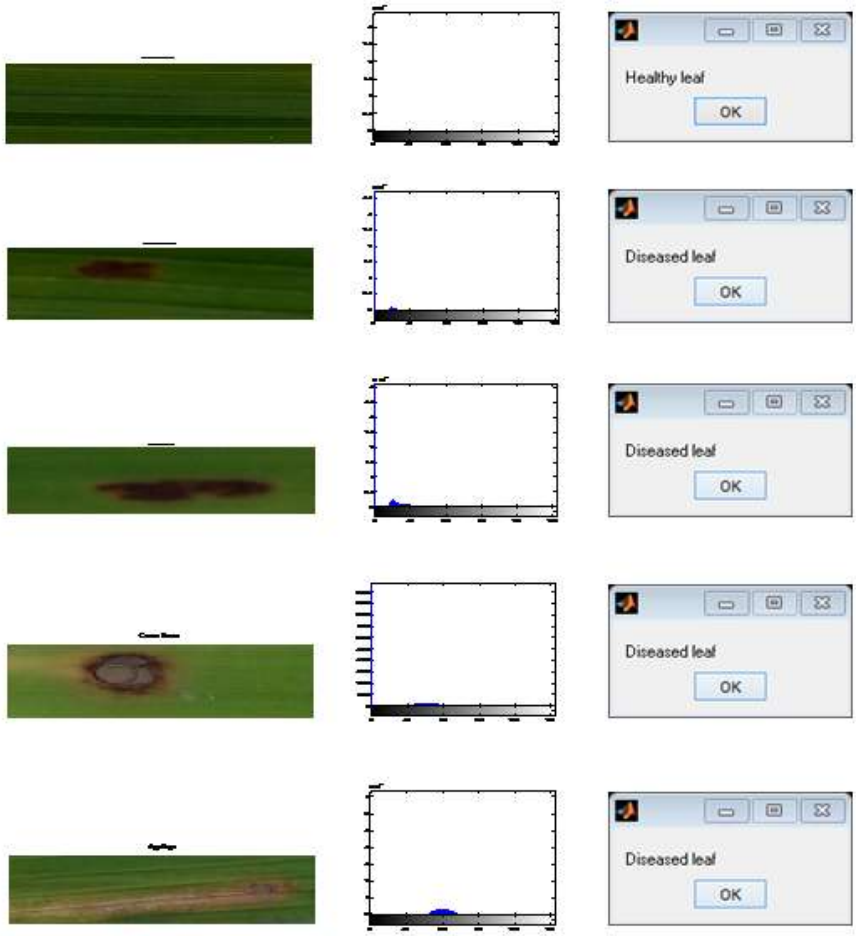

Figure 10:Original images and the Histogram plots of normal, bacterial leaf blight, brown spot, narrow brown spot and rice blast are given in (a)-(e), (f)-(j) respectively. And the results are given in (k)-(o)

The resultant images are used for the shape and color feature extraction. Classification of bacterial leaf blight, brown spot, narrow brown spot and rice blast diseases are carried out using SVM classifier. Here, 60 samples are used for classification purpose. For training 10 features are considered for each disease and for testing 5 samples for each disease. 70% accuracy has been achieved by using SVM classifier. TABLE 1 shows the resultant confusion matrix for classification of four diseases.

Fig 11: Segmented results of bacterial leaf blight, brown spot, narrow brown spot and rice blast respectively.

Table 1: Confusion Matrix for Classification

	Bacterial leaf blight	Brown spot	Narrow brown spot	Rice Balst
Bacterial leaf blight	5	0	0	0
Brown spot	2	2	0	1
Narrow brown spot	1	0	4	0
Rice Balst	2	0	0	3

VII. CONCLUSION

Identification of the symptoms of plant diseases by means of image processing techniques is of prime concern in the area of research. An introduction to the research in agriculture field and different types of diseases in rice leaf is given. The literature survey done in preprocessing techniques and segmentation of leaf disease detection and classification has been discussed. After applying the suitable preprocessing technique classification of normal and diseased leaf using histogram plot is presented. Shape features are extracted using PCA method and the color features are extracted by using color based grid moments. These features are combined and fed to the SVM classifier. 70% accuracy is achieved for four different diseases.

REFFERENCES

[1] Srivastava K.P, a text book of applied entomology New Delhi: Kalyani Publishers.

[2] Rice Doctor, International Rice Research Institute, Philipines, www.irri.org, 2003.

[3] Phadikar.S, Sil. J, Rice disease identification using pattern recognition techniques, IEEE 11th International Conference on Computer and Information Technology2008. ICCIT.

[4] J.N. Kapur, P.K. Sahoo, A.K.C. Wong, A new method for gray-level picture thresholding using the entropy of the histogram, Computer Vision Graphics Image Process. Vol. 29, pp.273-285, 1985

[5] P. Sanyal, U. Bhattacharya and S. K. Bandyopadhyay ,Color Texture Analysis of Rice Leaves Diagnosing Deficiency in the Balance of Mineral Levels Towards Improvement of Crop Productivity, IEEE 10th International Conference on Information Technology, pp. 85-90, 2007.

[6] Kurniawati, N.N. Abdullah, S.N.H.S. ; Abdullah, S. Investigation on Image Processing Techniques for Diagnosing Paddy Diseases, IEEE International Conference of Soft Computing and Pattern Recognition, SOCPAR '09. 4-7 Dec. 2009.

[7] K. J. Yoon and I.S. Kweon, Color Image Segmentation Considering the Human Sensitivity for Color Pattern Variations, Photonics Boston, SPIE, 2001, pp. 269-278.

[8] H. Tian, S.K. Lam and T. Srikanthan, 2003. Implementing Otsus Thresholding Process using Area-Time Efficient Logarithmic Approximation Unit, proc. Of ISCAS03, IV-21-IV-24.

[9] A.K. Jain, 1989. fundamental of digital image processing. NJ: Prentice Hall.

[10] Libo Liu and Guomin Zhou, Extraction of the Rice Leaf Disease Image Based on BP Neural Network. IEEE International Conference on Computational Intelligence and Software Engineering. CiSE 2009.

[11] Asfarian, A. Herdiyeni, Y.Rauf, A.Mutaqin, K.H, Paddy diseases identification with texture analysis using fractal descriptors based on fourier spectrum. IEEE Conference on Computer, Control, Informatics and Its Applications (IC3INA), 2013 International .